Regulatory Toxicology and Pharmacology 90 (2017) 170–184

Contents lists available at ScienceDirect

Regulatory Toxicology and Pharmacology

journal homepage: www.elsevier.com/locate/yrtph

Acute oral toxicity study of magnesium oxide nanoparticles and microparticles in female albino Wistar rats

Bhanuramya Mangalampalli [a, b], Naresh Dumala [a, b], Paramjit Grover [a, *]

[a] Toxicology Unit, Pharmacology and Toxicology Division, CSIR - Indian Institute of Chemical Technology, Hyderabad, Telangana 500007, India
[b] Academy of Scientific and Innovative Research, CSIR - Indian Institute of Chemical Technology, Hyderabad, Telangana 500007, India

ARTICLE INFO

Article history:
Received 10 January 2017
Received in revised form
1 September 2017
Accepted 5 September 2017
Available online 9 September 2017

Keywords:
Magnesium oxide nanoparticles
Wistar rats
Genotoxicity
Biodistribution
Antioxidant assays
Hematological alterations

ABSTRACT

Advancements in nanotechnology have led to the development of the nanomedicine, which involves nanodevices for diagnostic and therapeutic purposes. A key requirement for the successful use of the nanoparticles (NPs) in biomedical applications is their good dispensability, colloidal stability in biological media, internalization efficiency, and low toxicity. Therefore, toxicological profiling is necessary to understand the mechanism of NPs and microparticles (MPs). MgO NPs have attracted wide scientific interest due to ease of synthesis, chemical stability and unique properties. However, their toxic effects on humans should also be of concern with the increased applications of nano MgO. The present study was aimed to assess the toxicological potential of MgO NPs in comparison to their micron counterparts in female Wistar rats. Toxicity was evaluated using genotoxicity, histological, biochemical, antioxidant and biodistribution parameters post administration of MgO particles to rats through oral route. The results obtained from the investigation revealed that the acute exposure to the high doses of MgO NPs produced significant ($p < 0.01$) DNA damage and biochemical alterations. Antioxidant assays revealed prominent oxidative stress at the high dose level for both the particles. Toxicokinetic analysis showed significant levels of Mg accumulation in the liver and kidney tissues apart from urine and feces. Further, mechanistic investigational reports are warranted to document safe exposure levels and health implications post exposure to high levels of NPs.

1. Introduction

Nanomaterials (NMs) are been used in biomedical applications as cosmetics, food products, antibiotic products and therapeutic preparations (Sahoo et al., 2007; Zhang et al., 2012). Among these NMs, nanoparticles (NPs) have good dispensability, colloidal stability in biological media, high internalization efficiency, and produce lower toxicity (Zhang et al., 2008) than those of corresponding microparticles (MPs). The unique physicochemical properties of NPs are responsible for their increased cell permeability and increased quantum effects as a function of their size (Hochella et al., 2008; Ivask et al., 2015). The utilization of NPs in various fields has increased throughout the world exponentially. However, the concerns that deliberate or accidental human and environmental exposure to NPs may lead to significant adverse effects (Oberdörster et al., 2007) which are inevitable. To overcome debates and concerns, nanotoxicology has emerged to address toxicological impacts of engineering NPs and safe use for mankind and environment (Drobne, 2007). The fact that NPs have been eliciting biological responses resulting in cellular toxicity and genotoxicity than MPs was demonstrated in several studies with different NPs (Arnold, 2013; Chen et al., 2008; Singh et al., 2013b; Wang et al., 2007; Zhang et al., 2010). Therefore, toxicological profiling is necessary to predict the potential hazards associated with the exposure of these particles. Consequently, NPs are able to get entry into the body via inhalation, dermal and oral routes. Moreover, Most of the health hazards occur through the entry of the NPs into GI tract could be via accidental ingestion through varied sources such as at manufacturing industries, contact with nano-structured surfaces, or along with the drinking water or eating food contaminated with NPs (Ahamed et al., 2011).

Among the known metal oxides magnesium oxide (MgO) NPs have attracted wide scientific interest due to ease of synthesis, chemical stability, unique properties and extensive applications in various fields. The main applications of nano MgO in chemical industry as catalyst, synthesis of petro-chemical products, corrosion

* Corresponding author.
E-mail addresses: paramgrover@gmail.com, grover@iict.res.in (P. Grover).

http://dx.doi.org/10.1016/j.yrtph.2017.09.005
0273-2300/

Abbreviations

MgO NPs	Magnesium oxide nanoparticles
MgO MPs	Magnesium oxide microparticles
TEM	Transmission electron microscopy
DLS	Dynamic light scattering
LDV	Laser doppler velocimetry
XRD	X-ray diffraction
BET	Brunner–Emmett–Teller technique
OECD	Organization for economic co-operation and development
MNT	Micronucleus test
% PCE	Percentage of polychromatic erythrocytes
MN-PCE	Micronucleated polychromatic erythrocytes
ROS	Reactive oxygen species
ICP-OES	Inductively coupled plasma optical emission spectrometer
ANOVA	Analysis of variance

inhibitors, surface coatings, fuel additives, refractory fiber board and metallic ceramics (Krishnamoorthy et al., 2012; Moorthy et al., 2015). In the field of medicine, MgO NPs are being used in antacid preparations, detoxifying agents, bio molecular detection and diagnostics (Bertinetti et al., 2009; Martínez-Boubeta et al., 2010). Similarly, despite the wide applications of MgO nanoparticles, there is serious lack of knowledge related to their impact on human health and environment.

Very few investigations conducted with MgO NPs using *in vitro* and *in vivo* models revealed interesting and conflicting results. MgO NPs were tested for cytotoxicity against human umbilical vein endothelial cells (HUVECs) revealed that the treatment of these particles significantly enhanced the NO release and total antioxidation competence of the HUVECs. (Ge et al., 2011). However, these particles were least effective in inducing cytotoxic effects against human astrocytoma U87 cells (Lai et al., 2008) and human cardiac microvascular endothelial cells (HCMECs) (Sun et al., 2011). Another study reported on human liver epithelial cancer cell line revealed no significant genotoxic effects at the investigated concentrations (Kumaran et al., 2015). Ghobadian et al. (2015) studied on zebrafish embryos reported that these MgO NPs induced cellular apoptosis and intracellular ROS. An *in vivo* study conducted with MgO NPs on rats produced dose-dependent pulmonary toxicity after acute intratracheal instillation (Gelli et al., 2015). Another study reported reduction in total antioxidant capacity in serum of rats after acute intratracheal instillation of MgO NPs (Kiranmai and Reddy, 2013).

We are aware that the acute oral toxicity of MgO NPs and MPs in albino Wistar rats has not been previously investigated. *In vivo* studies for the toxicological evaluation of NPs are important because animal systems are extremely complicated and their interactions with biological systems could lead to novel immune response, metabolism patterns, biodistribution and clearance which provide useful information on likely health hazards assessment in mankind (Fischer and Chan, 2007). Three different doses (test groups) were used in the current investigation which ranged from least or no toxicity to highly toxic. The low dose of 100 mg/kg body weight (bw), was chosen to replicate probable human exposure as the workers unintentionally get exposed to the NPs through hands and to the mouth during manufacturing processes in work space (Singh et al., 2013b). Further, the highest dose of 1000 mg/kg bw, which showed symptoms of toxicity was chosen to see the effect when large quantities of NPs are released accidentally into the environment, and reach the human body (Kumari et al., 2014a).

The acute oral toxicity study was conducted as per Organization for Economic Co-Operation and Development (OECD) test guideline known as the “acute oral toxicity-fixed dose method” (OECD 420, 2001). The procedure provides information on the hazardous properties and allows the substance to be ranked and classified according to the Globally Harmonised System (GHS) for the classification of chemicals. As per the test guideline, the observation period is 14 days. It consisted of a sighting study and a main study. In the sighting study, single female rat was administered with 5, 50, 300 and 2000 mg/kg bw dose sequentially. The main study was conducted with the single acute dose of 2000 mg/kg (limit test). Histopathological studies were also carried in animals dosed with 3, 50, 300 and 2000 mg/kg bw. The above mentioned “acute toxicity study” was used to select the doses for further experiments consisting of genotoxicity, biochemical and biodistribution studies and were carried out with 100, 500 and 1000 mg/kg bw doses. The characterization of NPs is required before predicting the toxicity to biological components (Murdock et al., 2008). Hence, in current study, the NPs and MPs were characterized using transmission electron microscopy (TEM), dynamic light scattering (DLS), laser Doppler velocimetry (LDV), X-ray diffraction (XRD) and Brunner–Emmett–Teller (BET) analysis were measured.

Genotoxicity studies are intended to evaluate the effects of test chemicals on DNA/chromosome which may lead to oncogene activation or functional loss of tumor suppressor gene results in mutations and cancer inductions. The *in vivo* genotoxicity was studied using comet (Tice et al., 2000; OECD 489, 2014), micronucleus (MNT) (Schmid, 1975) and chromosomal aberration (CA) assays (Adler, 1984). The CA assay involves analysis of mitotically arrested metaphase cells for the presence of structural chromosomal alterations induced by the test compounds. The levels of aspartate aminotransferase (AST), alanine aminotransferase (ALT) and alkaline phosphatase (ALP) enzyme analysis has become a standard measure of hepatotoxicity. The presence of these markers in the blood in significant quantities suggests tissue damage (Ophardt, 2003). Therefore, these enzyme biomarkers were estimated to determine the functional status of liver and kidney upon oral exposure to MgO NPs and MPs. The present study also aimed to explore the oxidative stress induction ability of MgO particles. Hence, superoxide dismutase (SOD), catalase (CAT), glutathione (GSH), malondialdehyde (MDA) and Lactate dehydrogenase (LDH) levels were evaluated in serum, liver and kidney homogenates in the treated rats in comparison to controls. Further, hematology and serum markers were also estimated.

Histopathological examination is necessary to determine the morphological changes owing to NPs exposure and also for assessing the toxicological effects on liver, kidney, heart, spleen and brain (Reddy et al., 2017). NPs have different rates of absorption, persistence, distribution, accumulation, and elimination patterns when compared to MPs resulting in a potent interaction with animal models (Dumala et al., 2017). Metal content analysis is required to estimate the amount of Magnesium (Mg) that reached the target tissue or site after oral administration of NPs and MPs. Hence, the amount of metal content in rat's whole blood, liver, kidney, heart, brain, spleen, lungs, urine and feces was also analyzed using inductively coupled plasma optical emission spectrometry (ICP-OES) to estimate the uptake and retention of MgO particles and also for determining the anatomic fate, clearance and biological effect of these substances.

2. Materials and methods

2.1. Chemicals

MgO NPs (MgO < 50 nm, 99.9%, CAS No. 1309-48-4) were purchased from Sigma Chemical Co. Ltd (St Louis, MO, USA). MgO MPs (fine powder, 99.9%, GRM1031, CAS No. 1309-48-4) (according to the manufacture's data sheet) and all other chemicals were purchased from Himedia, Mumbai, India.

2.2. Characterization

The particles were characterized using TEM, BET, XRD, DLS and LDV analysis to evaluate the material size and morphology, surface area, crystal structure, size distribution, zeta potential and state of dispersion in Milli-Q water for the determination of average particle size of NPs and MPs using a TEM (JEM-2100, JEOL, Japan). Hundred particles showing the general morphology were measured from different fields of view. The specific surface area (m^2/g) of the particles was determined by N_2 adsorption–desorption measured at 77 K according to the BET protocol using a Quadrusorb-SI V 5.06 analyzer (M/S Quanta chrome Instruments Corporation, USA). The XRD pattern of the particles was documented on a Bruker AXS D-8 Advance powder X-ray diffractometer (Shimadzu, Japan). The instrument was operated at a current of 30 mA, voltage of 40 kV and utilizing a CuKα radiation ($\lambda = 1.5406$ Å). The size of the NPs and agglomerates was measured through DLS and LDV using a Malvern Zetasizer Nano-ZS (Malvern Instruments, UK. At the concentration of 40 μg/ml freshly prepared MgO NPs and MPs suspension in Milli-Q water was ultra sonicated using a probe sonicator (UP100H, Hielscher Ultrasonics GmbH, Teltow, Germany) for 10 min at 90% amplitude. The polydispersity index (PdI) was used to measure the different size ranges exist in the solution. The values of PdI scale lies in the range of 0–1, where the PdI scale value near to 0 indicates monodisperse and 1 indicates polydisperse state of the particles.

2.3. Animals

The animal model used for the study was female albino Wistar rats. They were procured from the National Institute of Nutrition (NIN), Hyderabad, India. The animals were 6–8 weeks old and had a weighs ranging from 120 to 140 g. The animals were housed in polypropylene cages, five animals kept per cage. The animals were given standard laboratory pellet diet and water *ad libitum*. They were kept at a humidity of 55–65%, temperature of 22 ± 3 °C and automated light cycles of 12 h light/12 h dark. The study design and experimental protocol was submitted to Institutional Animal Ethics Committee and the approval had a No. IICT/BIO/TOX/PG/25/06/2014/08.

2.4. Acute oral toxicity study-fixed dose method

The acute oral toxicity of MgO NPs and MPs were assessed by following OECD test guideline 420, known as the “acute oral toxicity-fixed dose method” (OECD 420, 2001).

2.5. Histopathological evaluation

Histopathological studies were conducted in the all visceral organs i.e. liver, kidneys, spleen heart and brain of rats after acute oral exposure to 5, 50, 300 and 2000 mg/kg bw of MgO NPs and MPs to assess the changes in the tissue anatomy. After sacrifice, the tissues were collected and washed with ice cold normal saline (0.9%) to remove debris or extraneous material. The tissues were fixed in formalin solution (10%). After the fixation, tissues were processed (Leica TP 1020) and embedded in paraffin blocks (Leica EG 1160). The paraffin blocks were sliced into 3 μm thick ribbons (Microm H 360) and placed on clean microscope slide. H & E dye was used for staining the tissue sections on a slide and analyzed for histological alterations using Nikon Eclipse E 80 microscope at ×400 magnification. A minimum of three slides per block were assessed for histological changes of the tissues.

2.6. Experimental design: genotoxicity, biochemical and bio distribution studies

MgO NPs and MPs were suspended in Milli-Q water, properly ultra sonicated (UP100H, Germany) and vortexed before treatment of the rats. For analysis of genotoxicity (comet, MN), biodistribution, biochemical and oxidative stress parameters, a total of 75 rats were taken and further divided into 5 groups such as control (Milli-Q water), low (100 mg/kg bw), medium (500 mg/kg bw), high (1000 mg/kg bw) dose groups and positive control (cyclophosphamide-CP) group at 24 and 72 h sampling periods post-acute exposure with MgO NPs and MPs. Further, a set of 75 rats were grouped in similar fashion for analysis of CAs at 18 h and 24 h sampling periods after acute oral exposure to MgO particles. Each group consists of 5 animals. The positive control group was kept as a standard for genotoxicity analysis. A dose of 40 mg/kg bw was injected intraperitonially 24 h before sacrifice in CP treated group. The doses were administered once using a suitable incubation cannula with volume 0.01 ml/g bw. The doses are selected on the basis of an initial range finding study. The lowest dose demonstrated slight adverse effects, whereas, highest dose was selected based on induction of a toxic effect without severe sufferings or mortality. All treated rats were sacrificed by cervical dislocation at different sampling periods.

2.7. Genotoxicity parameters

2.7.1. Comet assay

The alkaline comet assay was conducted in Wistar rats after oral acute exposure to MgO NPs and MPs at 24 h and 72 h sampling periods as per the method of Tice et al. (2000) and test guideline 489 (OECD 489, 2014). The whole blood was withdrawn in EDTA-coated tubes from retro-orbital plexus of rats. Comet assay in liver tissues was carried out according to Pant et al. (2014). The liver tissue were isolated from the rats after sacrificing at 24 h and 72 h sampling periods, minced and suspended at ~100 mg/ml in chilled homogenizing buffer (pH 7.5) and homogenized at 500–800 rpm. Cell viability was determined by the trypan blue exclusion assay (Pool-Zobel et al., 1994). Briefly, 10 μl of blood/cell suspension was mixed in 120 μl of 0.5% LMA in PBS and embedded in between the layers of NMA (0.75%) and LMA (0.5%) on a microscopic slide and spread uniformly with cover slip and allowed to solidify overnight at 37°C. The slides were kept for drying at 4 °C for 10 min. The cover slip was then removed and slides were immersed in chilled lysis buffer (2.5 M NaCl, 0.1 M Na_2 EDTA, 0.2 M NaOH, 1% Triton X-100, 10% DMSO, pH 10.0) for 10 h at 4 °C for facilitating alkaline unwinding of DNA, all slides were soaked for 20 min in alkaline buffer (10 M NaOH, 200 mM Na_2 EDTA, pH > 13.0) and then electrophoresis was performed at 25 V (or 300 mA) for 25 min. The neutralization of slides was done twice in 0.4 M tris buffer, pH 7.5, for 5 min and followed by methanol fixation. The slides were analyzed by staining with ethidium bromide (20 μg/ml) using a fluorescence microscope (Olympus, Shinjuku-ku, Tokyo, Japan) and scored for DNA damage blindly in order to avoid bias. Fifty randomly selected comets per slide (150 comets per rat) were analyzed to estimate the amount of DNA damage and expressed as

the percentage of DNA in the comet tail. Quantification of DNA breakage was carried out by using CASP software version 1.2.2 (Comet Assay Software, CaspLab) to calculate the amount of DNA damage and expressed as a percentage of DNA in the comet tail.

2.7.2. Micronucleus test (MNT)

The MNT in the rat bone marrow cells was carried out following the method described by Schmid (1975). The bone marrow cells were extracted from thigh bone of rats after acute oral exposure for 24 h and 72 h to MgO NPs and MgO MPs. The bone marrow was removed from both femurs by aspiration with hypotonic solution of 1% sodium citrate and centrifuged at 1000 rpm for 5 min to get a pellet. The pellet was resuspended in a drop of 1% sodium citrate and a smear was prepared on a microscope slide and allowed to dry in humidified air overnight. The MNT in peripheral blood lymphocytes (PBL) was performed according to the protocol described by Çelik et al. (2005) and test guideline 474 (OECD 474, 2014) with some modifications. Whole blood was collected from retro-orbital plexus of each rat at 24 h and 72 h after the treatment from each group. Smears were prepared on clean microscope slides and dried overnight in humidified air. The dried slides were fixed in methanol for 3 min and stained with 0.5% Giemsa for 5 min. Three slides were made for each animal at all sampling times and microscopically examined at ×1000 magnification for presence of MN. 2000 polychromatic erythrocytes (PCEs) per animal were selected from three slides and the frequencies of micro nucleated PCEs (MN-PCEs) and % PCE were recorded.

2.7.3. Chromosomal aberration assay

The method described by Alder et al. (1984) and test guideline 475 (OECD 475, 2014) was followed to carry out CA analysis in bone marrow cells at 18 h and 24 h sampling periods. For analysis of metaphase cells, cell division was arrested by a mitotic inhibitor, colchicine (0.02%), injected intraperitonially 2 h prior to sacrifice. The bone marrow was collected from femur and tibia by rinsing with hypotonic solution (0.56% potassium chloride) and centrifuged. Cells were then fixed in ice-cold Carnoy's solution (methanol: acetic acid, 3:1 v/v) until the pellets were clean. After overnight refrigeration, cells were centrifuged and resuspended in fresh fixative i.e. Carnoy's solution, dropped onto slides, dried and stained with Giemsa. Three slides for each animal were made by the flame-dried technique. Five hundred well spread metaphases per dose (100/animal) were selected to detect the presence of CAs. The mitotic index (MI) was determined with 1000 cells.

2.8. Hematological estimation

The red blood cells (RBC), white blood cells (WBC), hemoglobin (HGB), hematocrit (HCT) and mean corpuscular volume (MCV) were determined by using hematology analyzer ABX Micros ES 60 (HORIBA Medical, France).

2.9. Biochemical and oxidative stress parameters

Blood samples were collected from all the control and treated animals for complete blood picture and biochemical analysis as well. Blood was collected by puncturing the retro-orbital sinus into heparin-coated capillaries. Before taking the blood, animals were anaesthetized with an optimal cocktail of Xylazine and Ketamine to avoid pain/distress. A small amount (0.5 ml) of blood was collected in 10% EDTA coated vials for haematological parameters and serum was collected by centrifuging blood without any anticoagulant for biochemical analysis. The liver and kidney were quickly dissected, washed in ice-cold saline and then with buffer of pH 7.4 (0.15 M Tris-HCl), dried and weighed. Tissues were then homogenized in ice-cold sucrose (0.25 M) to make 10% homogenate (w/v) with a Miccra D-1 high speed tissue homogenizer. To get the supernatant, the homogenate was centrifuged at 12000 rpm for 10 min. Protein was determined in all treated and control samples as described by Lowry et al. (1951). The collected supernatants along with the serum were stored in −20 °C freezer until use for the biochemical analysis. Serum and tissue homogenates (liver and kidney) of treated and control samples were used to analyse the AST, ALT and ALP levels and estimation of lipid peroxidation, reduced GSH, catalase, SOD, LDH levels. All the biochemical and oxidative stress parameters were estimated after acute oral treatment with 100, 500 and 1000 mg/kg doses of MgO NPs and MPs at 24 and 72 h sampling periods using a spectrophotometer (Spectramax Plus, Molecular Devices, USA). Serum markers such as albumin, calcium, glucose, chloride, cholesterol, HDL cholesterol, triglycerides and creatinine were estimated by methods described in the diagnostic kit from Siemens Ltd. (Vadodara, Gujarat, India).

2.9.1. Aspartate aminotransferase and alanine aminotransferase activity

The activity of AST and ALT enzyme levels were measured in serum and tissue homogenates by followed the procedure by Yatzidis (1960). AST and ALT activities were expressed as U/ml in serum and U/mg protein for tissue (liver and kidney) homogenates.

2.9.2. Alkaline phosphatase activity assay

The activity of ALP was determined by following p-nitrophenyl phosphate method described in the diagnostic kit from Siemens Ltd. (Vadodara, Gujarat, India). This method utilizes p-nitrophenyl phosphate that is hydrolyzed to a yellow-colored product p-nitrophenol catalyzed by ALP and having absorbance at 405 nm (Spectra Max Plus; Molecular Devices). The rate of reaction is directly proportional to the enzyme activity. The enzyme activity was expressed as μmol/min/ml using the molar extinction coefficient of 18.75 mM^{-1} cm^{-1}.

2.9.3. Reduced glutathione (GSH) content

The reduced GSH content was analyzed in serum and tissue homogenates in according to the protocol of Jollow et al. (1974). The quantity of GSH present was expressed as U/ml in serum and U/mg protein for tissue (liver and kidney) homogenates.

2.9.4. Catalase

Catalase activity in serum and tissue homogenates was determined according to the protocol described by Aebi (1984). The enzyme activity was recorded at 240 nm and using a molar extinction coefficient of 43.6 M^{-1} cm^{-1}. The activity was expressed as U/ml in serum and U/mg protein for tissue (liver and kidney) homogenates.

2.9.5. Superoxide dismutase

SOD activity in the serum, tissue homogenates (liver and kidney) was carried out following the method described by Marklund and Marklund (1974). The rate of inhibition of pyrogallol auto-oxidation after the addition of enzyme extract was read at 420 nm. The amount of enzyme required to give 50% inhibition of pyrogallol auto-oxidation was considered as one unit of enzyme activity. The activity was expressed as U/ml in serum and U/mg protein for tissue (liver and kidney) homogenates.

2.9.6. Lactate dehydrogenase activity

The activity of LDH was estimated in the serum, homogenates of liver and kidneys according to the procedure described by McQueen (1972). In a quartz cuvette, required amounts of Sorensen phosphate buffer NADH, serum/homogenate was added. To this

mixture sodium pyruvate was added and mixed well. The absorbance was measured at 340 nm at 10 s interval for 2 min using a spectrophotometer. The LDH activity was expressed as μmol/h/ml in serum and μmol/h/mg protein for tissue (liver and kidney) homogenates using molar extinction coefficient of 6.3 mM^{-1} cm^{-1}.

2.9.7. Lipid peroxidation

Malondialdehyde (MDA) which is the end product of lipid peroxidation was measured in serum and tissue (liver and kidney) homogenates according to the procedure of Ohkawa et al. (1979) with slight modifications. The result of reaction among serum, tissue homogenates with thiobarbituric acid (TBA) and 15% of trichloroacetic acid (TCA) reagent formed TBA–MDA complex and read at 532 nm. The quantity of MDA was determined using a molar extinction coefficient of 1.56×10^5 M^{-1} cm^{-1} and expressed as nmol/ml in serum and nmol/mg protein of MDA formed/gm wet weight of tissue (liver and kidney).

2.10. Magnesium content analysis in tissues

The biodistribution study of acute dose of MgO NPs and MPs was carried out in female albino Wistar rats. The treated animals were placed in metabolic cages to collect the urine and feces samples along with control groups at sampling times of 24 h and 72 h after dosing. Rats were sacrificed through cervical dislocation and whole blood, liver, kidneys, heart, brain and spleen were collected. The samples were processed using the method of Gómez et al. (1997). Nitric acid digested (overnight) samples were heated at 80 °C for 10 h, and heated additionally heating at 130–150 °C for 30 min. Subsequently, perchloric acid (0.5 ml, 70%) was added, followed by heating at 130–150 °C for evaporating to dryness. Nitric acid (2%) was used to digest the dried sample and filtered with Whatman filter paper. The filtrate was made to a final volume of 5 ml with 2% nitric acid solution for ICP-OES analysis. The standard solution of Mg was serially diluted to 100, 50, 10, 1 ppm and wavelength of 418.66 nm was found to get intensity of samples. The Mg content in the samples was determined using ICP-OES (JY Ultima, JobinVyon, France).

2.11. Statistical analysis

The results were analyzed for the statistical significant changes between treated and control groups by two-way ANOVA. All results were expressed as mean and standard deviation (mean ± SD) of the mean. Multiple pair-wise comparisons were done using the Bonferroni posttest to verify the significance of positive response. Statistical analyses were performed using GraphPad Prism 5 Software package for windows (GraphPad Software, Inc., La Jolla, CA, USA). The statistical significance for all tests was set at $p < 0.05$.

3. Results

3.1. Characterization of MgO NPs and MgO MPs

The mean size of MgO NPs and MPs was found to be 52.97 ± 3.72 nm and 12.09 ± 2.5 μm respectively measured in random field using TEM (Fig. 1A and B). The hydrodynamic diameter and PdI of MgO NPs in Milli-Q water suspension obtained by DLS was 185.82 ± 23.65 nm and 0.555 respectively. The larger hydrodynamic diameter than the TEM size indicated that MgO NPs formed larger agglomerates in Milli-Q water suspension than in the dry state. Zeta potential (ζ) and electrophoretic mobility of MgO NPs in Milli-Q was quantified by LDV and found to be −11.6 mV and 0.542 (μm·cm)/(V·sec) respectively at pH 7.0 and is shown in Fig. 1C and D. The crystalline nature of NPs and MPs was hexagonal and cubic respectively by XRD analysis and diffraction peaks were consistent with standard database files (JCPDS card No. 780430 and 760667) (Fig. 1E and F). The specific surface area of MgO NPs and MPs was found to be 142.8 m^2/g and 43.88 m^2/g by BET analysis. In case of MgO MPs, the DLS and LDV data found to be out of the detection limit (Table 1).

3.2. Animal observation, food consumption, body weight and organ weight

Female Wistar rats were orally administered with the 5, 50, 300 and 2000 mg/kg bw doses of MgO NPs and MPs and no adverse effects and mortality were detected during 14 days observation period in sighting study. However, in main study rats treated with 2000 mg/kg bw of NPs showed dullness, irritation and moribund symptoms. Further, both MgO NPs and MPs treated rats showed a reduction in body weight gain, feed intake and organ weight profile (data not shown) but the loss was statistically non-significant. Percentage loss in feed intake and bw was in the range of 2.6–6.5% for NPs treated group and 1.5–3.4% for the MPs treated group when compared to controls. Mortality was not observed in rats treated with acute dose of 2000 mg/kg bw of MgO NPs and MPs. Hence, the acute toxicity of MgO NPs and MPs was greater than 2000 mg/kg bw ranking these substances into category V, as per guideline 420 (OECD 420, 2001) and the globally harmonized system.

3.3. Histopathological examinations

All the tissue sections were evaluated for any pathological changes as well as presence of any extraneous deposits. Liver tissues obtained from rats treated with a single dose of 2000 mg/kg of MgO NPs, showed tissue degeneration and necrosis, whereas, kidneys showed a focal tubular damage and swelling in the renal glomerulus. There were no morphological changes in spleen, heart and brain tissues with 2000 mg/kg bw (data not shown). The sections of liver and kidneys of control rats are shown in Fig. 2A and B, whereas sections of rats received 2000 mg/kg bw dose are shown in Fig. 2 C&D. The rats exposed to 5, 50 and 300 mg/kg bw of MgO NPs and all doses of MgO MPs exhibited the normal architecture histology. Moreover, extraneous material deposition was not found in the examined tissues.

3.4. Genotoxicity analysis

3.4.1. Comet assay

The findings of the comet assay after acute oral treatment with the 100, 500 and 1000 mg/kg doses of MgO NPs and MPs at various sampling times are depicted in Fig. 3. Cell viability of PBL and liver cells of all the samples ranged from 85 to 95% (data not shown). There was a significant ($p < 0.01$) increase in % tail DNA in the PBL and liver cells of rats at 1000 mg/kg dose of MgO NPs at 24 h and 72 h sampling times. At the 500 mg/kg bw dose, a significant ($p < 0.05$) % tail DNA was observed at both the sampling periods in liver cells, whereas, in PBL at 24 h only. However, no significant increase in % tail DNA was observed at 100 mg/kg bw of MgO NPs and all doses of MgO MPs in comparison to control group. On the other hand, the mean % tail DNA in CP treated rats was significant ($p < 0.01$) when compared with the control.

3.4.2. Micronucleus test (MNT)

The MNT in bone marrow and PBL was performed after acute oral treatment with 100, 500 and 1000 mg/kg bw of MgO NPs and MPs in female rats at 24 h and 72 h sampling times and the results are shown in Table 2. The data indicated at 1000 mg/kg bw dose of

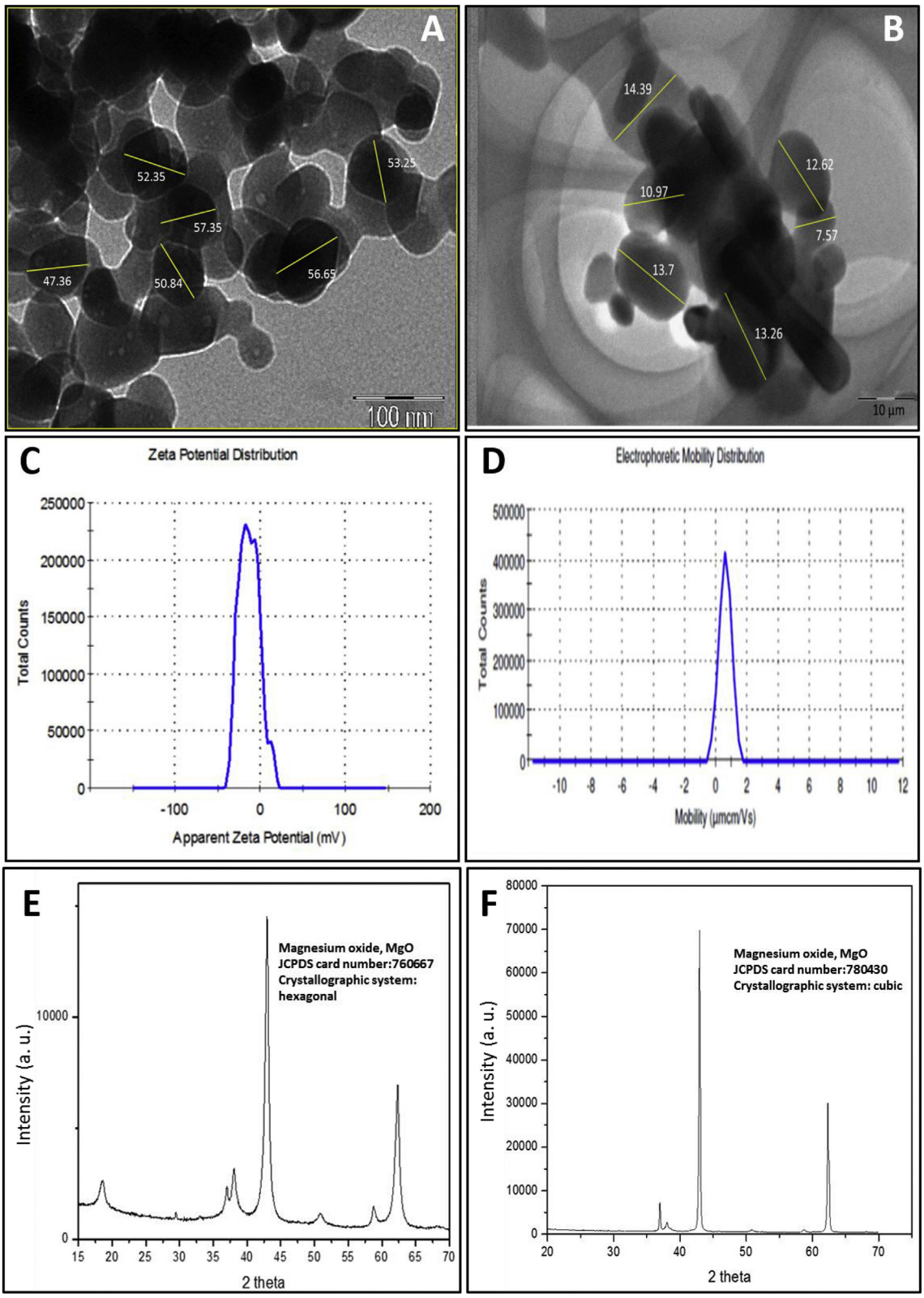

Fig. 1. Transmission electron microscopy (TEM) image of (A) Magnesium oxide nanoparticles (MgO NPs) and (B) MgO microparticles (MPs); (C) zeta potential (D) electrophoretic mobility of MgO NPs in Milli-Q water for characterization of particles; (E and F) XRD patterns of MgO NPs and MPs, respectively.

MgO NP treated rats, MN-PCEs frequency in bone marrow cells was significant ($p < 0.05$) at 24 h sampling time. The percentage PCEs in bone marrow cells decreased in dose dependent manner but significant ($p < 0.01$) at 24 h and 72 h sampling period. In PBL cells, dose dependent significant ($p < 0.05$) increase in MN-PCEs frequency was at 1000 mg/kg of MgO NPs, whereas, percent PCEs

Table 1
Characterization of Magnesium oxide nanoparticles (MgO NPs) and microparticles (MPs).

Particles	Size using TEM	DLS		LDV			Surface area (m^2g^{-1})
		Average diameter (nm)	PDI	Zeta Potential (mv)	Electrophoretic mobility (μm·cm)/(V·sec)	pH	
MgO NPs (nm)	52.97 ± 3.72	185.82 ± 23.65	0.555	−11.6	0.542	7.0	142.8
MgO MPs (μm)	12.09 ± 2.5	ND	ND	ND	ND	7.0	43.88

MgO NPs and MPs were dispersed in Milli-Q water and mixing was done via probe sonication for 10 min just before estimations.
PdI = Polydispersity Index.
DLS = Dynamic Light Scattering.
LDV = Laser Doppler Velocimetry.
ND = not detectable.

shown significant ($p < 0.05$) at 500 and 1000 mg/kg bw dose of MgO NP treated rats at both sampling times. On the other hand, MgO MPs did not produce any significant MN-PCEs and %PCE frequency at the investigated doses at 24 h and 72 h sampling times. The positive control group rats treated with CP induced a highly significant ($p < 0.01$) on both MN-PCEs frequency % PCEs when compared to treated and control group of rats.

3.4.3. Chromosomal aberration assay (CA)

The results of CA assay were examined after the acute oral exposure of MgO NPs and MPs at various doses (100, 500 and 1000 mg/kg bw) of bone marrow cells in female Wistar rats at 18 h and 24 h sampling periods and shown in Table 3 (A&B). MI did not reveal any statistical differences between the treated and control group of rats. The MgO NPs induced significant ($p < 0.01$) CAs at 1000 mg/kg bw at both time periods of exposure. Moreover, there was a dose-dependent increase in numerical and structural changes (gaps, breaks, minutes and acentric fragments) were observed in MgO NPs treated bone marrow cells. The increase in aneuploidy was less significant ($p < 0.05$) at both 1000 and 500 mg/kg bw doses. However, there were no changes in polyploidy level and reciprocal translocations in any of treated groups. However, reciprocal translocations were observed only in CP treated groups but not in MgO NPs and MPs treated groups.

3.5. Hematological estimations

The hematological results revealed that MgO NPs and MPs treated rats showed the levels of HGB, RBC, PLT and HCT were reduced, while WBC levels were elevated in a dose dependent manner compared to control at 24 h sampling period and results were statistically significant at high dose ($p < 0.01$). Apart from the highest dose of MgO NPs, no other dose caused an observable change in the hematological parameters (Table 5).

3.6. Biochemical and oxidative stress parameters

Biochemical parameters were determined in the female Wistar rats after acute oral exposure to 100, 500, 1000 mg/kg bw doses of MgO NPs and MPs in serum (Table 4A) and tissue (liver and kidney) homogenates (Table 4B and C) at 24 h and 72 h sampling times. The acute doses of MgO NPs induced significant ($p < 0.01$) increase in AST and ALT activity in serum at the 1000 mg/kg. Moreover, in liver and kidney homogenates the enzyme levels were increased at all the three doses tested (100, 500, and 1000 mg/kg) at 24 h sampling period. A dose dependent increased level of ALP in serum, tissue homogenates at 24 h and 72 h sampling times upon MgO NPs exposure.

Oxidative stress parameters include GSH, SOD, CAT, LDH and MDA. In serum, tissue homogenates the reduced GSH content was inhibited in a dose-dependent manner compared with controls. The significant ($p < 0.01$) inhibition observed at 1000 mg/kg dose of the MgO NPs treated groups at 24 h and 72 h sampling times. SOD and CAT levels were also reduced in a dose-dependent fashion in all tested concentrations and significant ($p < 0.05$) in serum, and ($p < 0.01$) at 1000 mg/kg MgO NPs treated rats intissue homogenates in both sampling times. LDH levels were significantly enhanced ($p < 0.01$) at 1000 mg/kg in serum, whereas, in tissue homogenates they were significant ($p < 0.05$) at 500 mg/kg and ($p < 0.01$) at 1000 mg/kg MgO NPs treated rats in both sampling periods. The enhanced level of MDA was found to be significant ($p < 0.01$) at 1000 mg/kg bw of MgO NPs in the serum and tissue homogenates in both sampling periods. Moreover, at 100 mg/kg of MgO NPs and all doses of MgO MPs the changes in biochemical enzyme levels were non-significant compared to control group. Serum biochemical markers such as albumin, calcium, glucose, chloride, cholesterol, HDL cholesterol, triglycerides and creatinine were evaluated in serum of the treated rats and the changes in respective markers were significant at high dose of NP administered group of rats (Table 6).

3.7. Biodistribution of MgO NPs and MPs

The biodistribution analysis of Mg content after acute oral exposure of MgO NPs and MPs with various doses (100, 500 and 1000 mg/kg bw) in female Wistar rats was carried out in various tissues. Liver, kidneys, spleen, heart, brain and blood along with urine and faeces were collected and processed for Mg content by ICP-OES analysis. The results are shown in Fig. 4. The maximum accumulation of Mg was found in liver and next in kidney and blood. The dose dependent bioaccumulation of Mg was clearly evident and the order of accumulation of Mg was liver > kidneys > blood > spleen > heart > brain. After 24 h, the Mg concentration was started to decline in a time-dependent manner. This indicated that as the day passed the concentration of particles got diluted. The significant amount of Mg excreted in urine at all doses of MgO NPs treated rats and was found to be dose and time dependent. However, there was no significant removal of Mg through urine in MgO MPs treated group. Moreover, in feces, the maximum amount of Mg particles got cleared significantly in MPs treated group than NPs treated group and clearance was rapid from 24 to 72 h. Hence, MP treated rats showed more significant excretion of Mg content in the faces when compared to NP treated rats and control groups.

4. Discussion

MgO NPs have wide range of advantages across the fields and gained scientific interest in recent years due to the simple process of synthesis, high chemical stability and unique properties.

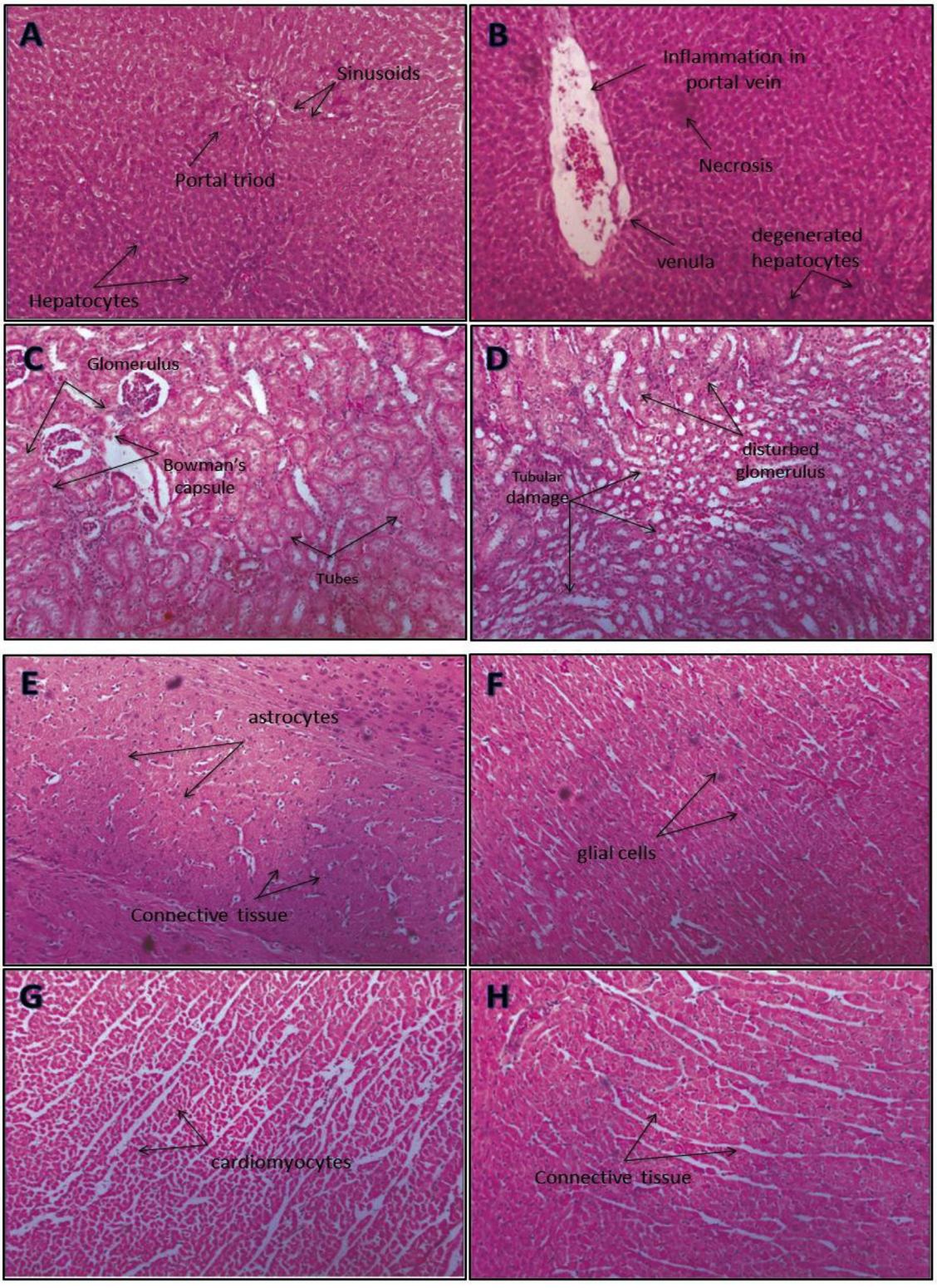

Fig. 2. Photomicrograph of the rats tissues after acute oral treatment with 2000 mg/kg bw MgO NPs (A) (C) (E) (G) showing normal architecture of liver, kidney, brain and heart, (B) showing tissue degeneration of liver tissue (D) focal tubular damage and degenerated glomerulus (F) (H) showing treated brain and heart tissues (no significant damage) at ×400 magnification (H and E staining).

However, the literature on MgO NPs exposure and their health consequences via oral route is limited. Hence, the aim of the study was to assess the genotoxic, hematological, biochemical and biodistribution patterns of MgO NPs and compare it with their MPs after acute oral administration to female albino Wistar rats.

Characterization of the NPs is important to study the toxicity induced by engineered NPs for understanding the possible toxicological implications upon acute oral exposure (Braakhuis et al.,

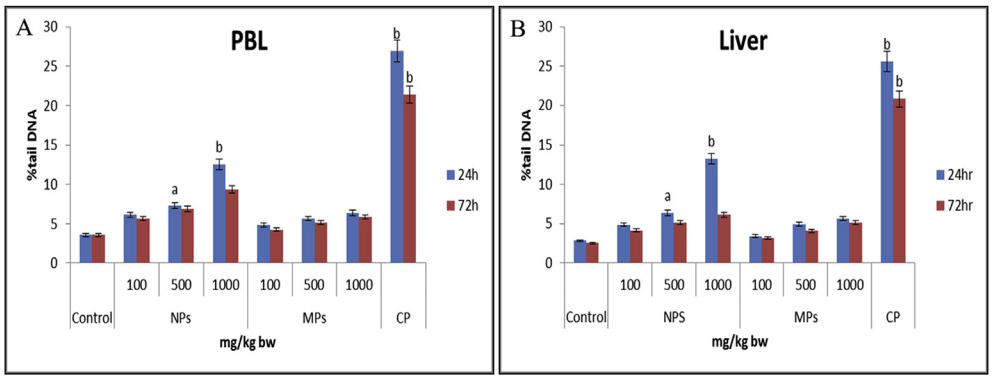

Fig. 3. The *in vivo* comet assay of MgO NPs and MPs. (A) Mean % tail DNA in PBL and (B) Mean % tail DNA in liver after 24 and 72 h of oral treatment in female Wistar rats. Milli-Q water (control), cyclophosphamide (CP) as positive control, Data represented as mean ± SD., significantly different from control at $^{a}p < 0.05$, $^{b}p < 0.01$, n = 5.

Table 2
The frequency of MN-PCEs and percent PCEs in female rat bone marrow cells and peripheral blood cells treated orally with different doses of MgO NPs and MPs at 24 and 72 h.

Treatment	Dose (mg/kg)	Bone marrow cells				Peripheral blood cells			
		24 h		72 h		24 h		72 h	
		MN-PCEs frequency	% PCEs	MN-PCEs frequency	% PCEs	MN-PCEs frequency	% PCEs	MN-PCEs frequency	% PCEs
Control[A]	Milli-Q	3.66 ± 1.18	40.3 ± 1.83	4.11 ± 1.92	31.4 ± 1.67	2.02 ± 1.16	4.33 ± 1.53	1.94 ± 1.92	4.24 ± 1.67
MgO NPs	100	3.86 ± 1.72	39.3 ± 1.53	4.98 ± 0.64	32.4 ± 1.74	2.16 ± 1.74	3.87 ± 0.63	2.18 ± 0.68	3.84 ± 1.84
	500	5.5 ± 1.14	37.4 ± 2.89	6.2 ± 1.34	28.3 ± 2.18	2.35 ± 1.19	3.52 ± 0.88	2.52 ± 1.74	3.38 ± 2.91
	1000	**7.4 ± 1.86**[a]	**35.5 ± 2.27**[b]	**7.3 ± 0.61**[a]	**25.76 ± 2.56**[b]	**4.16 ± 1.08**[a]	**2.23 ± 1.92**[a]	**3.97 ± 0.96**[a]	**2.16 ± 0.76** [a]
MgO MPs	100	3.46 ± 1.11	40.56 ± 3.82	4.26 ± 0.73	30.16 ± 3.24	2.12 ± 1.19	4.16 ± 1.12	1.86 ± 0.83	3.96 ± 0.28
	500	4.6 ± 0.57	38.5 ± 3.43	5.1 ± 0.87	29.6 ± 2.54	2.43 ± 0.76	3.78 ± 0.53	2.31 ± 0.87	3.65 ± 0.58
	1000	5.2 ± 1.28	37.6 ± 2.52	5.42 ± 1.84	27.6 ± 3.43	2.62 ± 1.14	3.83 ± 1.63	2.34 ± 1.62	4.18 ± 1.62
CP[B]	40	**21.3 ± 4.12**[b]	**28.0 ± 3.68**[b]	**22.4 ± 3.58**[b]	**23.5 ± 2.48**[b]	**19.28 ± 1.76** [b]	**1.86 ± 0.36** [a]	**16.12 ± 0.47** [b]	**2.18 ± 1.48** [a]

Data represented as mean ± standard deviation, Values which are in bold significantly different from control at $^{a}p < 0.05$ and $^{b}p < 0.01$, (n = 5). [A]Milli-Q water (negative control). [B]Cyclophosphamide (positive control); n = 5 animals per group.

Table 3A
Chromosome aberrations and percent mitotic index observed in bone-marrow cells of female Wistar rats treated acute with different doses of MgO NPs and MgO MPs (18 h).

Dose(mg/Kg/BW)	M.I (%)	Chromosomal aberrations							Abberent cells (%)	Total Cytogenic Changes	TA+ Gaps	TA-Gaps
		Numerical Aberrations		Structural aberrations								
		Aneuploidy	Polyploidy	Gaps	Breaks	Minutes	Acentric fragments	Reciprocal Translocations				
[A]Control	5.4 ± 0.42	0.31 ± 0.43	0.0 ± 0.0	0.43 ± 0.65	0.52 ± 0.87	0.18 ± 0.37	0.23 ± 0.76	0.0 ± 0.0	0.62 ± 0.43	1.67 ± 0.33	1.36 ± 0.42	0.93 ± 0.32
MgO NPs												
100	5.14 ± 0.76	1.93 ± 0.32	0.0 ± 0.0	0.96 ± 0.32	0.75 ± 0.89	0.58 ± 1.4	0.42 ± 1.3	0.0 ± 0.0	1.87 ± 0.32	4.64 ± 1.23	2.71 ± 0.54	1.75 ± 0.41
500	4.88 ± 0.97	**2.97 ± 0.87**[a]	0.0 ± 0.0	1.18 ± 0.65	0.67 ± 0.16	0.88 ± 0.23	0.71 ± 0.87	0.0 ± 0.0	2.61 ± 1.66	**7.08 ± 1.54**[b]	3.44 ± 1.3	2.26 ± 0.52
1000	**3.66 ± 0.53**[a]	**4.12 ± 1.2**[b]	0.0 ± 0.0	**2.1 ± 1.1**[a]	1.6 ± 0.65	1.5 ± 0.32	1.3 ± 1.4	0.0 ± 0.0	3.4 ± 0.76	**11.22 ± 2.4**[b]	**7.1 ± 2.32**[b]	**5 ± 0.77**[a]
MgO MPs												
100	5.21 ± 0.64	0.62 ± 0.76	0.0 ± 0.0	0.71 ± 0.43	0.24 ± 0.52	0.18 ± 0.76	0.29 ± 0.59	0.0 ± 0.0	1.07 ± 0.65	2.04 ± 0.76	1.42 ± 0.33	0.71 ± 0.14
500	4.62 ± 0.83	0.89 ± 1.3	0.0 ± 0.0	1.17 ± 0.76	0.32 ± 0.2	0.43 ± 0.2	0.56 ± 0.24	0.0 ± 0.0	1.44 ± 0.68	2.77 ± 0.33	1.88 ± 0.56	0.71 ± 0.22
1000	4.51 ± 0.95	2.11 ± 1.6	0.0 ± 0.0	1.33 ± 0.56	0.76 ± 0.43	0.81 ± 0.42	0.44 ± 0.21	0.0 ± 0.0	1.86 ± 0.75	**5.45 ± 1.65**[a]	3.34 ± 1.47[a]	2.01 ± 0.54
[B]CP	**3.14 ± 0.42**[a]	**33.34 ± 5.5**[b]	**1.96 ± 0.9** [b]	**2.5 ± 0.63**[b]	**10.7 ± 3.54**[b]	**13.16 ± 3.87**[b]	**12.35 ± 3.13**[b]	**1.30 ± 2.4** [b]	**25.76 ± 5.42**[b]	**65.31 ± 5.65**[b]	**31.97 ± 3.65**[b]	**29.47 ± 3.22**[b]

Values which are in bold significantly different from control at [a] = $p < 0.05$, [b] = $p < 0.01$. One hundred metaphases were analyzed per animal; n = 5 animals per group. Total cytogenetic changes = NA and structural aberrations. Abbreviations: MI, mitotic index; data represented as mean ± standard deviation; TA, total aberrations = structural aberrations. [A] Negative control (Milli-Q water). [B] Cyclophosphamide (40 mg/kg bw).

2014). Appropriate analytical methods for assessing average particle size, shape, specific surface area, the state of aggregation and surface charge are necessary to gather veritable data on NPs properties (López-Heras et al., 2014). Hence, MgO NPs and MPs were characterized using TEM, BET, XRD, DLS and LDV measurements. It is generally considered that the size of the particles is main factor for their toxicity, as smaller the size, the particles are more toxic (Asare et al., 2012). The larger specific surface area of MgO NPs (142.8 m^2/g) than the MPs (43.88 m^2/g), allow them easily penetrate into cells and get transferred into the bloodstream to reach different target sites, including nerve cells (Gheshlaghi et al., 2008).

The oral administration of different doses of MgO NPs and MPs in rats did not cause any adverse pathological changes in 14day

Table 3B
Chromosome aberrations and percent mitotic index observed in bone-marrow cells of female Wistar rats treated acute with different doses of MgO NPs and MgO MPs (24 h).

Dose (mg/Kg)	M.I (%)	Chromosomal aberrations							Abberent cells (%)	Total cytogenic changes	TA± Gaps	TA-Gaps
		Numerical aberrations		Structural aberrations								
		Aneuploidy	Polyploidy	Gaps	Breaks	Minutes	Acentric fragments	Reciprocal translocations				
[A]Control	5.32 ± 0.36	0.51 ± 0.31	0.0 ± 0.0	0.63 ± 0.65	0.53 ± 0.87	0.28 ± 0.37	0.21 ± 0.76	0.0 ± 0.0	0.82 ± 0.53	2.16 ± 0.87	1.65 ± 0.43	1.02 ± 0.42
MgO NPs												
100	5.5 ± 0.67	2.3 ± 0.46	0.0 ± 0.0	1.16 ± 0.32	0.79 ± 0.89	0.58 ± 1.4	0.41 ± 1.3	0.0 ± 0.0	1.76 ± 0.42	5.24 ± 1.13	2.94 ± 1.18	1.78 ± 0.54
500	4.98 ± 0.91	**3.27 ± 0.36**[a]	0.0 ± 0.0	1.28 ± 0.65	0.93 ± 0.16	0.78 ± 0.23	0.64 ± 0.87	0.0 ± 0.0	2.98 ± 1.76	**6.9 ± 1.34**[a]	3.63 ± 0.25	2.35 ± 1.09
1000	**3.16 ± 0.51**[a]	**5.72 ± 1.2**[a]	0.0 ± 0.0	2.5 ± 1.1	1.9 ± 0.65	1.5 ± 0.32	1.4 ± 1.4	0.0 ± 0.0	**3.52 ± 0.82**[a]	**13.02 ± 1.42**[b]	**7.3 ± 1.5**[b]	4.8 ± 1.22
MgO MPs												
100	5.11 ± 0.62	0.82 ± 0.62	0.0 ± 0.0	0.81 ± 0.43	0.43 ± 0.52	0.68 ± 0.76	0.39 ± 0.59	0.0 ± 0.0	1.37 ± 0.45	3.13 ± 0.87	2.31 ± 1.1	1.5 ± 0.76
500	4.62 ± 0.38	1.33 ± 1.23	0.0 ± 0.0	1.47 ± 0.76	0.69 ± 0.25	0.33 ± 0.2	0.46 ± 0.24	0.0 ± 0.0	1.58 ± 0.68	4.28 ± 1.11	2.95 ± 0.87	1.48 ± 0.42
1000	4.46 ± 0.59	2.13 ± 1.46	0.0 ± 0.0	1.53 ± 0.56	1.04 ± 0.43	0.81 ± 0.42	0.64 ± 0.21	0.0 ± 0.0	2.43 ± 0.85	**6.15 ± 1.32**[a]	4.02 ± 1.37[a]	2.49 ± 0.62
[B]CP	**3.51 ± 0.48**[a]	**37.27 ± 2.54**[b]	**2.63 ± 0.64**	**8.2 ± 2.33**[b]	**12.76 ± 3.54**[b]	**13.6 ± 2.87**[b]	**12.35 ± 3.13**[b]	**1.41 ± 0.38**[b]	**28.76 ± 4.34**[b]	**88.22 ± 6.75**[b]	**50.95 ± 4.92**[b]	**42.75 ± 3.65**[b]

Values which are in bold significantly different from control at [a] $= p < 0.05$, [b] $= p < 0.01$. One hundred metaphases were analyzed per animal; n = 5 animals per group. Total cytogenetic changes = NA and structural aberrations. Abbreviations: MI, mitotic index; data represented as mean ± standard deviation; TA, total aberrations = structural aberrations. [A] Negative control (Milli-Q water). [B] Cyclophosphamide (40 mg/kg bw).

Table 4A
Effects of MgO NPs and MPs on serum biochemical and oxidative stress parameters in female Wistar rats treated after acute oral exposure at 24 h and 72 h.

Treatment	Dose(mg/kg bw)	AST(μmol/h/ml)		ALT(μmol/h/ml)		ALP(μmol/h/ml)		Catalase(U/ml)	
		24hr	72hr	24hr	72hr	24hr	72hr	24hr	72hr
Control	Milli Q	1.9 ± 0.25	0.97 ± 0.16	0.35 ± 0.15	0.29 ± 0.12	215 ± 14.12	210 ± 14.31	121.4 ± 11.32	111.4 ± 14.34
MgO NPs	100	2.11 ± 0.3	1.01 ± 0.24	0.44 ± 0.14	0.33 ± 0.12	220 ± 15.24	215 ± 15.31	114.4 ± 15.67	95.2 ± 16.76
	500	2.32 ± 0.52	1.11 ± 0.26	0.58 ± 0.18	0.46 ± 0.13	235 ± 16.43	222 ± 18.2	**98.3 ± 4.63**[a]	**88.5 ± 11.45**[a]
	1000	**2.91 ± 0.82**[a]	**1.91 ± 0.58** [a]	**0.72 ± 0.3**[b]	**0.65 ± 0.25**[b]	**243 ± 15.20**[b]	**235 ± 18.26**[a]	**84.7 ± 9.65**[b]	**74.2 ± 10.42**[b]
MgO MPs	100	2.12 ± 0.85	1.38 ± 0.26	0.42 ± 0.12	0.35 ± 0.14	218 ± 16.21	212 ± 14.27	119.7 ± 17.35	105.11 ± 13.54
	500	2.32 ± 0.37	1.42 ± 0.76	0.55 ± 0.15	0.48 ± 0.16	228 ± 14.31	219 ± 14.24	102.2 ± 12.66	98.4 ± 11.31
	1000	2.55 ± 0.82	1.64 ± 0.68	**0.62 ± 0.23**[a]	0.54 ± 0.25	235 ± 15.26	229 ± 14.51	**98.1 ± 10.5**[a]	94.2 ± 15.3

Treatment	Dose(mg/kg bw)	SOD(U/mg Protein)		MDA(nmol/ml)		GSH(U/ml)		LDH(μmol/h/ml)	
		24hr	72hr	24hr	72hr	24hr	72hr	24hr	72hr
Control	Milli Q	7.5 ± 1.43	7.3 ± 1.33	1.95 ± 0.21	1.35 ± 0.41	3.73 ± 0.31	2.61 ± 0.32	7.21 ± 1.2	7.11 ± 1.34
MgO NPs	100	6.9 ± 1.76	5.6 ± 1.43	2.17 ± 0.4	1.51 ± 0.35	3.62 ± 0.28	2.46 ± 0.42	7.35 ± 1.35	7.25 ± 1.45
	500	6.1 ± 1.64	5.4 ± 1.45	**2.74 ± 0.5**[a]	2.05 ± 0.45	3.52 ± 0.43	2.26 ± 0.35	8.81 ± 1.55	8.17 ± 1.42
	1000	5.8 ± 1.54	**4.7 ± 1.64**[b]	**3.39 ± 0.6**[b]	**3.07 ± 0.45**[b]	**2.98 ± 0.31**[b]	**2.08 ± 0.32**[a]	**10.2 ± 1.33**[b]	**9.8 ± 1.15**[b]
MgO MPs	100	7.2 ± 1.53	6.8 ± 1.32	2.21 ± 0.26	1.49 ± 0.3	3.56 ± 0.39	2.48 ± 0.38	7.8 ± 1.67	6.7 ± 1.56
	500	6.6 ± 1.52	6.23 ± 1.34	2.59 ± 0.42	**2.15 ± 0.6**[a]	3.45 ± 0.43	2.35 ± 0.39	8.95 ± 1.36	8.31 ± 1.54
	1000	6.21 ± 1.34	5.87 ± 1.76	2.65 ± 0.85	**2.54 ± 0.65**[b]	3.24 ± 0.37	2.15 ± 0.28	8.5 ± 1.65	8.1 ± 1.4

Data represented as mean ± standard deviation. Values which are in bold significantly different from control at [a] $p < 0.05$, [b] $p < 0.01$; n = 5 animals per group.

sighting study period. However, histopathological analysis of MgO NPs treated rats at 2000 mg/kg dose showed spaces between hepatocytes and tissue degeneration in liver and swelling in the renal glomerulus in kidney. Further, no morphological alterations in the spleen, heart and brain were observed when compared with the control. The acute oral toxicity study has revealed NP induced toxic effects at high dose without any severe distress symptoms and mortality. In contrast, MPs did not show toxicity at all test concentrations. A study investigated on histopathological examination of rat lungs after exposed with MgO NPs showed a dose-dependant infiltration of interstitial lymphocytes, peribronchiolar lymphocytic infiltration, and dilated and congested vessels indicating the pulmonary toxicity Gelli et al. (2015). Further, a few more studies on of Fe_2O_3 NPs and NiO NPs have documented the hepatic and kidney tissue alterations in the rats post acute oral exposure (Reddy et al., 2017; Dumala et al., 2017).

Genotoxicity is considered as one of the important parameters for assessing toxicity of NPs exposure. From the decades, comet assay has been used for the genotoxicity assessment of potential toxicants. The results of comet assay showed an increase in % tail DNA in PBL and liver cells of rats treated with MgO NPs in a dose dependent manner and the increase was significant at 1000 mg/kg bw dose at both 24 h and 72 h sampling periods when compared with control group. Moreover, a non-significant increase in % tail DNA in PBL and liver cells of rats received MgO MPs at all doses and sampling times was recorded. The gradual reduction in the percentage tail DNA with time may be due to the action of complex DNA repair mechanism (Karlsson, 2010). Recent studies have shown the significant DNA damage in PBL and liver cells after acute oral treatment with metal oxide NPs by comet assay in rats (Kumari et al., 2014a; Chinde et al., 2017; Dumala et al., 2017). The bone marrow and PB MNT results have revealed a significant increase in MN frequency at 1000 mg/kg bw dose of MgO NPs at 24 and 72 h sampling times. The results of the current study suggested the occurrence of clastogenic events i.e. impairment in cell cycle progression which may be associated with NP toxicity. The percentage PCEs calculated in the NP-treated groups did not show any significant change in comparison to the control group, indicating that cell death had not occurred in any of the treated groups. The total cytogenetic changes revealed a significant dose dependent increase in

Table 4B
Effects of MgO NPs and MPs on liver biochemical and oxidative stress parameters in female Wistar rats treated after acute oral exposure at 24 h and 72 h.

Treatment	Dose(mg/kg bw)	AST(μmol/h/mg)		ALT(μmol/h/mg)		ALP(μmol/h/mg)		Catalase(U/mg)	
		24hr	72hr	24hr	72hr	24hr	72hr	24hr	72hr
Control	Milli Q	1.45 ± 0.25	1.1 ± 0.16	0.24 ± 0.12	0.26 ± 0.1	218 ± 16.32	216 ± 15.29	200.2 ± 14.16	200.5 ± 14.54
MgO NPs	100	0.76 ± 0.3	1.17 ± 0.24	0.36 ± 0.11	0.29 ± 0.15	222 ± 14.36	215 ± 15.23	194.1 ± 13.76	184.14 ± 13.92
	500	1.98 ± 0.52	1.23 ± 0.26	0.41 ± 0.2	0.38 ± 0.12	239 ± 15.28	232 ± 15.26	189.1 ± 18.35	178.4 ± 16.35
	1000	**2.61 ± 0.68** [a]	**1.69 ± 0.38** [a]	**0.66 ± 0.15**[b]	0.42 ± 0.12	**254 ± 16.31**[b]	**241 ± 15.36**[a]	**168.1 ± 15.21**[b]	**172.2 ± 14.54**[a]
MgO MPs	100	1.88 ± 0.5	1.12 ± 0.18	0.31 ± 0.12	0.25 ± 0.14	225 ± 14.27	219 ± 13.31	191.2 ± 14.54	198.1 ± 14.31
	500	2.08 ± 0.97	1.24 ± 0.76	0.35 ± 0.2	0.29 ± 0.16	235 ± 17.24	225 ± 15.71	183.1 ± 13.77	189.4 ± 14.65
	1000	2.22 ± 0.92	1.36 ± 0.68	0.36 ± 0.12	0.3 ± 0.14	**241 ± 16.38**[a]	231 ± 18.27	178.3 ± 21.3	181.6 ± 13.98

Treatment	Dose(mg/kg bw)	SOD(U/mg Protein)		MDA(nmol/mg)		GSH(U/mg)		LDH(μmol/h/mg)	
		24hr	72hr	24hr	72hr	24hr	72hr	24hr	72hr
Control	Milli Q	23.5 ± 2.43	21.6 ± 2.87	1.67 ± 0.2	1.59 ± 0.3	18.5 ± 2.93	18.1 ± 2.82	11.74 ± 2.1	11.46 ± 1.78
MgO NPs	100	21.4 ± 2.65	20.8 ± 2.43	1.83 ± 0.32	1.79 ± 0.41	17.5 ± 1.93	16.6 ± 2.54	13.8 ± 2.16	12.67 ± 2.32
	500	**19.2 ± 2.77**[a]	18.6 ± 2.65	2.43 ± 0.36	2.27 ± 0.34	16.9 ± 2.31	15.5 ± 1.45	**15.27 ± 2.34**[a]	13.22 ± 2.43
	1000	**17.8 ± 2.55**[b]	**16.6 ± 2.54**[b]	**3.85 ± 0.42**[a]	**3.32 ± 0.56**[a]	**13.8 ± 1.43**[b]	**13.2 ± 1.6**[b]	**16.8 ± 2.12**[b]	**15.16 ± 2.54**[a]
MgO MPs	100	22.2 ± 2.43	21.8 ± 2.26	1.71 ± 0.31	1.69 ± 0.26	17.7 ± 1.62	16.7 ± 1.57	12.87 ± 1.84	11.87 ± 2.43
	500	21.8 ± 2.24	20.6 ± 2.34	2.12 ± 0.28	2.03 ± 0.43	16.5 ± 1.49	15.8 ± 1.552	13.54 ± 2.42	13.76 ± 2.65
	1000	20.1 ± 2.14	19.6 ± 2.69	2.57 ± 0.39	2.04 ± 0.42	**15.2 ± 2.35**[a]	**14.8 ± 2.31**[a]	14.34 ± 2.35	12.6 ± 2.65

Data represented as mean ± standard deviation. Values which are in bold significantly different from control at [a] $p < 0.05$, [b] $p < 0.01$; n = 5 animals per group.

Table 4C
Effects of MgO NPs and MPs on Kidney biochemical and oxidative stress parameters in female Wistar rats treated after acute oral exposure at 24 h and 72 h.

Treatment	Dose(mg/kg bw)	AST(μmol/h/mg)		ALT(μmol/h/g)		ALP(μmol/h/mg)		Catalase(U/ml)	
		24hr	72hr	24hr	72hr	24hr	72hr	24hr	72hr
Control	Milli Q	0.45 ± 0.24	0.44 ± 0.38	0.23 ± 0.11	0.19 ± 0.12	220 ± 15.29	215 ± 15.21	203.5 ± 14.2	202.7 ± 14.33
MgO NPs	100	0.51 ± 0.21	0.45 ± 0.31	0.33 ± 0.12	0.25 ± 0.14	226 ± 14.23	221 ± 14.25	193.5 ± 3.42	185.4 ± 13.55
	500	0.56 ± 0.22	0.51 ± 0.17	0.41 ± 0.16	0.32 ± 0.2	233 ± 15.32	227 ± 18.42	188.7 ± 16.35	**177.5 ± 18.8**[a]
	1000	**0.98 ± 0.14**[b]	0.75 ± 0.22	**0.54 ± 0.21**[b]	0.4 ± 0.38	**252 ± 15.43**[b]	**247 ± 16.26**[b]	**174.7 ± 13.16**[b]	**166.5 ± 13.54**[b]
MgO MPs	100	0.47 ± 0.15	0.42 ± 0.18	0.22 ± 0.12	0.23 ± 0.16	225 ± 15.41	221 ± 16.26	191.7 ± 13.98	182.5 ± 14.12
	500	0.52 ± 0.2	0.47 ± 0.18	0.32 ± 0.12	0.25 ± 0.14	235 ± 14.4	229 ± 17.31	186.4 ± 14.22	**179.4 ± 18.2**[a]
	1000	0.56 ± 0.12	0.38 ± 0.16	0.41 ± 0.21	0.33 ± 0.18	243 ± 18.46	231 ± 16.23	**178.76 ± 18.35**[a]	**172.3 ± 17.25**[b]

Treatment	Dose(mg/kg bw)	SOD(U/mg Protein)		MDA(nmol/mg)		GSH(U/mg)		LDH(μmol/h/mg)	
		24hr	72hr	24hr	72hr	24hr	72hr	24hr	72hr
Control	Milli Q	13.8 ± 2.33	12.3 ± 1.23	1.74 ± 0.31	1.62 ± 0.36	17.5 ± 2.73	16.9 ± 2.68	10.8 ± 1.3	10.67 ± 1.33
MgO NPs	100	13.2 ± 1.82	11.6 ± 2.44	1.64 ± 0.26	1.54 ± 0.28	16.6 ± 1.31	15.4 ± 2.39	13.98 ± 2.83	12.34 ± 2.54
	500	11.1 ± 1.54	9.87 ± 2.54	**2.66 ± 0.39**[a]	2.13 ± 0.64	15.8 ± 2.54	14.1 ± 2.49	**14.87 ± 2.43**[a]	13.65 ± 2.54
	1000	**10.5 ± 1.76**[a]	**8.65 ± 1.55**[b]	**3.62 ± 0.49**[b]	**3.05 ± 0.41**[b]	**12.9 ± 1.49**[b]	**10.5 ± 1.75**[b]	**15.42 ± 2.66**[b]	**14.89 ± 2.76**[a]
MgO MPs	100	13.6 ± 1.65	12.76 ± 1.56	1.75 ± 0.37	1.58 ± 0.48	16.2 ± 1.49	15.3 ± 1.63	11.65 ± 2.45	12.76 ± 2.12
	500	12.8 ± 1.87	10.67 ± 2.66	2.24 ± 0.42	1.98 ± 0.45	15.9 ± 1.56	14.9 ± 2.31	12.8 ± 2.22	13.28 ± 2.86
	1000	11.5 ± 1.54	9.88 ± 1.76	**2.53 ± 0.41**[b]	2.12 ± 0.29	14.7 ± 1.85	**13.5 ± 1.74**[a]	**14.2 ± 2.54**[a]	14.3 ± 2.55

Data represented as mean ± standard deviation. Values which are in bold significantly different from control at [a] $p < 0.05$, [b] $p < 0.01$; n = 5 animals per group.

Table 5
Effects of MgO NPs and MPs on Hematological findings of female albino Wistar rats treated after acute oral exposure.

Parameters	Control	MgO NPs			MgO MPS		
		100 mg/kg	500 mg/kg	1000 mg/kg	100 mg/kg	500 mg/kg	1000 mg/kg
White Blood Cells (WBC) (10^3/μl)	7.16 ± 2.85	7.2 ± 0.2	8.3 ± 0.43	**9.8 ± 0.34**[a]	7.98 ± 0.5	8.48 ± 0.3	**8.96 ± 0.32**[a]
Red Blood Cells (RBC)(10^6/μl)	2.27 ± 0.15	2.75 ± 0.3	3.07 ± 0.4	**3.85 ± 0.43**[a]	2.68 ± 0.8	3.21 ± 0.87	3.66 ± 0.76
Hemoglobin (HGB)(gm/dl)	12.76 ± 1.96	13.1 ± 2.54	15.2 ± 1.2	**16.9 ± 2.1**[a]	12.92 ± 0.66	13.72 ± 0.76	14.74 ± 0.65
Hematocrit (HCT)%	13.3 ± 1.06	15.6 ± 3.2	**20.6 ± 2.1**[a]	**23.4 ± 3.1**[a]	17.46 ± 06	19.18 ± 0.5	**22.14 ± 0.6**[a]
Mean Corpuscular Volume (MCV) (μ/m^3)	55 ± 4.56	61 ± 5.1	64 ± 2.54	**73 ± 3.21**[b]	58.6 ± 1.2	59.8 ± 1.6	**67.8 ± 1.7**[a]

Data represented as mean ± standard deviation. Values which are in bold significantly different from control at [a] $p < 0.05$, [b] $p < 0.01$; n = 5 animals per group.

the rats which received MgO NPs. It was interesting to note that the increase in aberrant cells at high dose levels was due to aneuploidy effects. This might also explain why positive micronuclei were also seen at the high dose level as micronuclei are often the result of aneuploidy. The observed aneuploidy was may be due to interference of these MgO NPs with the cell division apparatus (Hashimoto et al., 2010). Further, the cytogenetic changes resulting in changes of chromosome copy number (aneuploidy) upon treatment with MgO particles might also be due to a spontaneous mechanism to remove extra DNA or during normal development from progenitor cells (Shimizu, 2011). Moreover, the interactions of NPs with chromosomes may lead to the formation of acentric fragments and mal-segregation at anaphase resulting in MN formation. However, it has been difficult to explain the exact relationship between aneuploidy and chromosomal instability because in addition to complex aneuploidy, they carry a wide variety of genetic and

Table 6
Effects of MgO NPs and MPs on biochemical parameters in female albino Wistar rats treated after acute oral exposure at 24 h.

TESTS	Control	MgO NPs			MgO MPs		
		100 mg/kg	500 mg/kg	1000 mg/kg	100 mg/kg	500 mg/kg	1000 mg/kg
Albumin (mg/dl)	2.61 ± 0.77	3.3 ± 0.12 (-26.43%)	3.49 ± 0.11 **(-33.71%)**[a]	3.55 ± 0.4 **(-34.09%)**[a]	2.95 ± 0.15 (-13.02%)	3.34 ± 0.85 (-27.90%)	3.37 ± 0.75 **(-29.11%)**[a]
Calcium (mg/dl)	10.52 ± 0.13	9.37 ± 1.07 (-10.93%)	8.37 ± 1.15 (-11.43%)	7.67 ± 0.6 **(-14.09%)**[a]	8.52 ± 2.14 (-19.01%)	8.08 ± 1.14 (-23.19%)	7.84 ± 1.5 (-25.47%)
Glucose (mg/dl)	80 ± 2.7	70.3 ± 2.12 (-17.12%)	65.4 ± 4.13 (-25.25%)	50.9 ± 2.13 **(-42.62%)**[b]	75.7 ± 4.7 (-23.87%)	71 ± 4.14 (-19.75%)	58.7 ± 3.75 (-56.62%)
Chloride (mEq/day)	94.6 ± 2.78	95.41 ± 4.13 (-4.2%)	101.83 ± 3.7 (12.23%)	107.95 ± 5.84 **(18.34%)**[a]	100 ± 5.64 (9.78%)	101.2 ± 5.56 (17.92%)	106.2 ± 4.12 **(27.14%)**[a]
Cholesterol (mg/dl)	94.82 ± 1.76	104.59 ± 5.77 (11.60%)	113.5 ± 5.1 **(29.70%)**[a]	137.1 ± 6.88 **(39.78%)**[b]	91.26 ± 4.98 (-5.30%)	96.95 ± 6.44 (2.11%)	117.2 ± 5.7 (23.60%)
HDL Cholesterol (mg/dl)	69.5 ± 1.94	72.1 ± 3.7 (6.30%)	62.1 ± 3.7 (-15.40%)	55.78 ± 3.13 **(-34.65%)**[b]	68.94 ± 4.13 (-3.76%)	61.31 ± 4.41 (-5.70%)	59.05 ± 3.35 **(-21.60%)**[a]
Tri glycerides (mg/dl)	59.7 ± 0.32	104.85 ± 5.43 (58.22%)	134.3 ± 4.84 **(76.88%)**[a]	165.6 ± 6.29 **(112.68%)**[b]	60.89 ± 5.7 (4.80%)	82.6 ± 4.29 (23.35%)	95.6 ± 2.29 **(68.68%)**[a]
Creatinine (mg/dl)	1.95 ± 1.48	3.19 ± 1.44 (59.69%)	3.88 ± 1.6 **(89.69%)**[a]	4.33 ± 1.43 **(104.54%)**[b]	2.97 ± 1.17 (34.58%)	3.01 ± 1.5 (58.35%)	3.67 ± 1.14 **(88.2%)**[a]

Data represented as mean ± standard deviation. Values which are in bold significantly different from control at [a] $p < 0.05$, [b] $p < 0.01$; n = 5 animals per group.

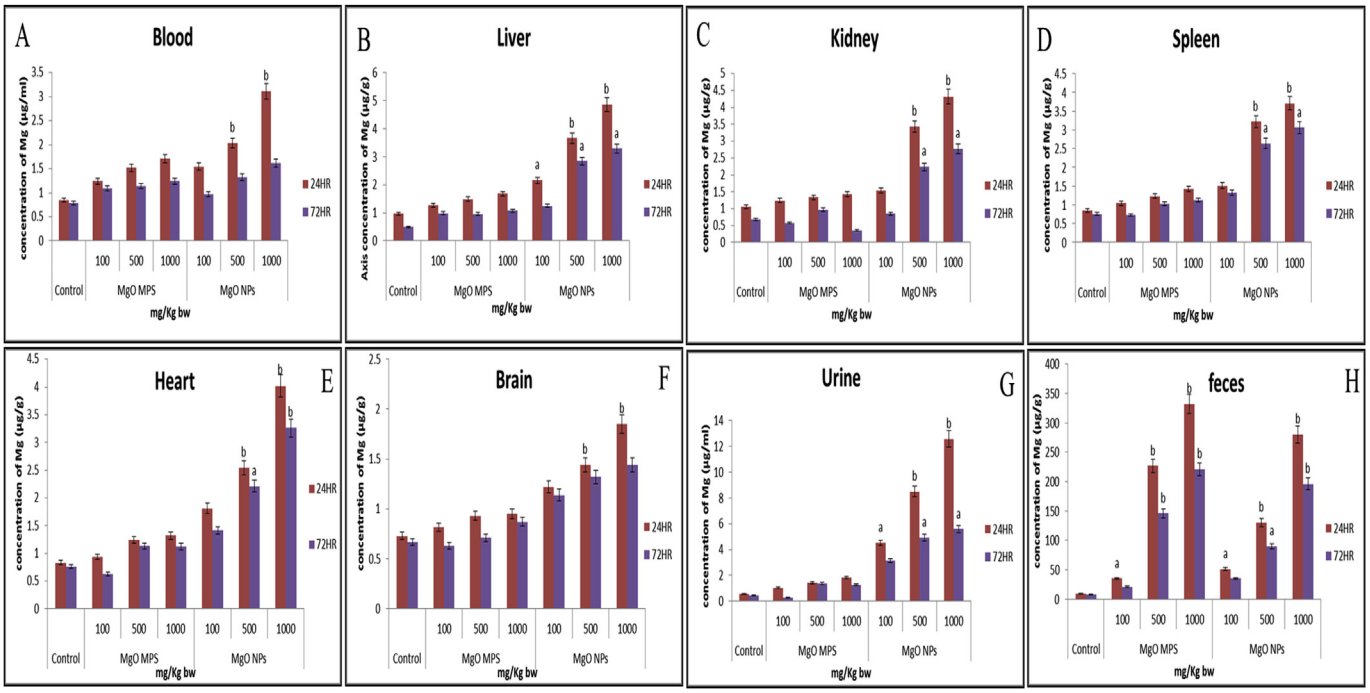

Fig. 4. Tissue biodistribution of Mg measured by ICP-OES in (A) blood; (B) liver; (C) kidney (D) spleen; (E) heart; (F) brain; (G) urine and (H) feces of rats after 24 and 72 h of treatment with MgO NPs and MPs in female Wistar rats. Significantly different from control at [a]$p < 0.05$, [b]$p < 0.01$, n = 5.

epigenetic alterations compared to normal karyotype. Nevertheless, there are several studies in experimental models such as yeast, plants and mammalian cells which elucidated the alliance of aneuploidy and chromosomal instability (Potapova et al., 2013).

A study with TiO_2 NPs treated orally to mice, induced DNA damage in bone marrow and liver cells (Sycheva et al., 2011). Another study by Singh et al. (2013c) with iron oxide NPs and MPs revealed a dose dependent DNA damage by comet assay and significant total cytogenetic changes and % MN-PCE at the higher doses administered to the rats which are in accordance with this study.

Hematological parameters were assessed to examine the physiological state of the rats after acute oral exposure to MgO NPs and MPs. It was found that the rats dosed with NPs showed significant decrease in HGB, RBC, PLT and HCT and a marginally significant increase in WBC at the highest dose (1000 mg/kg bw) investigated. The reduction in RBC, HCT and HGB might be due to the interference of NPs in the process of erythropoiesis (Morsy et al., 2016). The increase in WBC count indicated that the innate defence system was activated in the body (Gui et al., 2011). A study conducted hematological analysis after treatment with TiO_2 NPs in rats and showed a significant reduction in RBC and HCT levels and enhancement in MCV, PLT, MPV and WBC at higher doses. Moreover, abnormally shaped red cells, some of them having micronuclei, hyper segmented neutrophil nuclei were also documented (Grissa et al., 2015).

The significant quantity of aminotransferases in the blood suggests tissue damage (Ophardt, 2003). In the current study, significant elevated levels of AST and ALT in the serum, liver and kidney homogenates of rats were noted upon exposure of NPs at highest

dose. It suggests probable injury to liver and kidney tissues upon NP exposure (Adeyemi et al., 2015). Moreover, a traceable amount of ALP in the bloodstream at high dose also recorded which indicates probable effect of NP exposure. However, significant increases were observed at 24 and 72 h after treatment with high dose of NPs. Similar results were found in serum and tissue homogenates of rats after acute oral exposure with metal oxide NPs (Kumari et al., 2013; Parivar et al., 2016; Dumala et al., 2017).

The present study was also focused on the determination of oxidative stress induction capabilities of MgO NPs and MPs at the different sampling periods. NP induced ROS may cause significant damage in cells, which lead to oxidation of proteins and unbalancing the redox potential in cellular environment (Liou and Storz, 2010). MDA levels were significantly elevated in NP-treated rats after 24 h and 72 h sampling times at 1000 mg/kg bw in the serum and tissue homogenates suggesting that NPs might have induced free radical generation. These free radicals readily attack the polyunsaturated fatty acids leads to the destruction of membrane lipids and the result in MDA release, especially dangerous for the viability of cells and tissues (Mylonas and Kouretas, 1999). After MgO NP treatment, the GSH levels were decreased at the 24 and 72 h sampling times at high dose in the serum, tissue (liver and kidney) homogenates possibly due to increased utilization of GSH in neutralizing the free radicals generated. The levels of MDA may rise and GSH levels might decline when excessive ROS are produced signifying that the treated rats suffered an oxidative stress condition.

SOD considered as the first line of defense against toxicity to neutralize free radicals (Lobo et al., 2010). In this study, MgO NPs strongly inhibited the SOD activity at the 24 h and 72 h sampling times at high dose in serum and tissue homogenates. Decreased SOD activity and increased number of leukocytes were indicators of enhanced ROS level, resulting in tissue impairment (Thomas et al., 2014). The H_2O_2 production increases in cells to neutral superoxide radicals released (Hussein et al., 2016). Further, H_2O_2 is converted to hydroxyl radicals via enzymatic reactions. These are potent free radicals to cause oxidative damage at the cellular levels. CAT activity was decreased at the 24 h and 72 h sampling times at 1000 mg/kg in the serum, liver and kidney homogenates suggesting possibly high levels of H_2O_2 production (He et al., 2016). Enhancement in the LDH levels in the serum, liver and kidneys after MgO NP exposure at the 24 h and 72 h sampling times at 1000 mg/kg bw was recorded which might be due to NPs induced cell membrane damage and injuries to the tissues (Bahadar et al., 2016). A study reported elevated levels of MDA and depletion of SOD, catalase, and total antioxidant status upon inhalation exposure of MgO NPs to rats, which strongly correlated to the ROS generation resulting oxidative stress (Kiranmai and Reddy, 2013). Another study by Gelli et al. (2015) reported increased levels of LDH and ALP enzymes which were investigated after inhalation exposure with MgO NPs in BAL fluid of rats instillation causes lowering of antioxidant capacity by induction of oxidative stress indicating the dose dependent lung toxicity. Mahmoud et al. (2016) observed that MgO NPs showed oxidative damage and cytotoxicity through decreased cell metabolic activity in different cell lines. Some earlier investigations of oral MgO NPs exposure, reported ROS production which lead to interference with the antioxidant defense system resulting in oxidative stress (Yamakoshi et al., 2003; Shrivastava et al., 2016; Heringa et al., 2016). Further, several more *in vitro* studies were also reported NP induced ROS production can cause cell death in different types of cultured cells (Sun et al., 2011; Krishnamoothy et al., 2012; Pirela et al., 2016; Kongseng et al., 2016).

On the other hand, there are some reports of positive effects of MgO NPs available in literature. A study reported a considerable decrease in oxidative stress markers ROS and MDA level in rat pancreatic islets after 24 h exposure of MgO NPs. Furthermore, these NPs can induce antiapoptotic, antioxidative, and antidiabetic effects in rat pancreatic islets (Moeini-Nodeh et al., 2017). Another study found Mg in its metal form reduced LPO level in cadmium-induced oxidative stress in rats by effecting glutathione peroxidase enzyme (Buha et al., 2012). Furthermore, Mg has neuroprotective effects and reduced LPO after spinal cord injury in rats (Süzer et al., 1999).

Toxicokinetic study of the MgO NPs and MPs helps in better understanding of the movement of the particles in physiological systems after the acute oral administration in rats. Biodistribution analysis of the NPs helps in prediction and understanding of the probable mechanism of toxicity. In the present study, a significant biodistribution of MgO NPs occurred in different tissues of treated rats. Our data revealed that maximum accumulation was in the liver followed by kidneys, heart, spleen, lungs and blood. The distribution was in a dose- and time-dependent order, as the amount absorbed increased with higher the dose administered. The incorporation rate of Mg in different organs of rats ranged from 0.5 to 270 μg/g of tissue for MgO NPs and 1–340 μg/g of tissue for MgO MPs. As liver is the primary site of metabolism and kidney being the excretory organ they got the maximum exposure to the particles apart from other vital organs. A little quantity of Mg was found in the urine when compared to the quantity of Mg found in the feces. The significant levels of Mg in urine from the MgO NP-treated group was observed when compared to the control group, whereas, MP-treated rats showed extremely high levels of Mg in the feces. The significant increase in the tissue concentration of Mg might be the factor responsible for the alterations in various parameters including biochemical profile. The study by Lee et al. (2016) reported maximum accumulation of Cu in the liver and kidneys, excretion in urine and feces of Cu NP-treated mice, in contrast to Cu MPs. Moreover, MP treated rats showed extremely high levels of Cu in the feces. Similar kinetic study in mice with TiO_2 NPs and CeO_2 NPs demonstrated the retention of NPs in the liver, spleen, kidneys (Kumari et al., 2014b; Wang et al., 2007) and was in accordance with this study.

The possible mechanisms of genotoxicity may be either by direct interaction of NPs with the genetic material cause micronuclei formation or could attack DNA base guanine and form mutagenic 8-OHdG lesions DNA fragmentation and aberrations in chromosomes (Singh et al., 2013a) or by indirect damage from NPs-induced ROS. From the results of the current investigation it could be anticipated that the mechanism of toxicity was oxidative stress, which was evidenced by ROS profile.

5. Conclusions

It is clear from our results that MgO NPs produced significant toxicity at higher doses as compared to MgO MPs with genotoxicity, biochemical, histopathology and biodistribution parameters. Further, NPs showed more bioaccumulation than MPs at the same dose level and the accumulation was size, dose and time dependent manner. The DNA damage and histological alterations are evident from the results of the current study. Moreover, toxicokinetic results of the particles in the present study suggest that MgO NPs and MgO MPs showed significant difference in the biodistribution of Mg in rats. Our results showed elevated levels of MDA, depletion of GSH, CAT, SOD, are strongly correlated to ROS generation and thus indicating induction of oxidative stress. In our investigation high doses were included to get genotoxicity and biochemical changes of the NPs after absorption in to the rats. We do not conclude that these materials should not be used for biological benefits; rather sufficient care should be taken while using the MgO NPs for

biomedical purposes as it may lead to undesired health consequences. Moreover, future investigations are suggested to get clear cut mechanistic illustration of the toxicity produced and better understanding of the possible health hazards associated with over exposure regimens of NPs.

Funding

This study was financially supported by CSIR Emeritus Scheme to Dr. Paramjit Grover (Grant No. 21(1021)/16/EMR-II) from Human Resource Development Group, Extramural Research Division, Council of Scientific and Industrial Research, India.

Authors' contributions

All authors have contributed to the work and participated in preparation of the manuscript.

Conflict of interest statement

There is no conflict of interest related to this research.

Acknowledgments

We express our sincere thanks to the Director, IICT, Hyderabad for providing funds and facilities to execute this study. Bhanuramya Mangalampalli (SRF) is grateful to University Grants Commission. Further, Naresh Dumala (SRF) and Dr. Paramjit Grover (CSIR-Emeritus Scientist) are grateful to Council of Scientific and Industrial Research, India for the award of fellowships.

Appendix A. Supplementary data

Supplementary data related to this article can be found at http://dx.doi.org/10.1016/j.yrtph.2017.09.005.

Transparency document

Transparency document related to this article can be found online at http://dx.doi.org/10.1016/j.yrtph.2017.09.005.

References

Adeyemi, O.T., et al., 2015. Alkaline phosphatase (ALP), aspartate aminotransferase (AST) and alanine aminotransferase (ALT) activities in selected tissues of rats fed on processed atlantic horse mackerel (Trachurus trachurus). Adv. Biosci. Biotechnol. 6, 139–145.
Adler, I., 1984. Cytogenetic Tests in Mammals. Mutagenicity Testing: A Practical Approach. IRL Press, Oxford, England, UK, pp. 275–306.
Aebi, H., 1984. Catalase in vitro. Methods Enzym. 105, 121–126.
Ahamed, M., et al., 2011. Oxidative stress mediated apoptosis induced by nickel ferrite nanoparticles in cultured A549 cells. Toxicology 283 (2-3), 101–108.
Arnold, L., 2013. Random Dynamical Systems. Springer Science & Business Media.
Asare, N., et al., 2012. Cytotoxic and genotoxic effects of silver nanoparticles in testicular cells. Toxicology 291 (1–3), 65–72.
Bahadar, H., et al., 2016. Toxicity of nanoparticles and an overview of current experimental models. Iran. Biomed. J. 20 (1).
Bertinetti, L., et al., 2009. Surface characteristics of nanocrystalline apatites: effect of Mg surface enrichment on morphology, surface hydration species, and cationic environments. Langmuir 25, 5647–5654.
Braakhuis, H.M., et al., 2014. Physicochemical characteristics of nanomaterials that affect pulmonary inflammation. Part. Fibre Toxicol. 11 (1).
Buha, Aleksandra, et al., 2012. Effects of oral and intraperitoneal magnesium treatment against cadmium-induced oxidative stress in plasma of rats. Archives Industrial Hyg. Toxicol. 63 (3), 247–254.
Çelik, A., et al., 2005. The evaluation of micronucleus frequency by acridine orange fluorescent staining in peripheral blood of rats treated with lead acetate. Mutagenesis 20, 411–415.
Chen, S.-S., et al., 2008. Attenuation of oxidative stress after varicocelectomy in subfertile patients with varicocele. J. urology 179 (2), 639–642.
Chinde, S., et al., 2017. Toxicological assessment of tungsten oxide nanoparticles in rats after acute oral exposure. Environ. Sci. Pollut. Res. 24 (15), 13576–13593.
Drobne, Damjana, 2007. Nanotoxicology for safe and sustainable nanotechnology. Arh. za Hig. rada i Toksikol. 58 (4), 471–478.
Dumala, N., et al., 2017. Genotoxicity study of nickel oxide nanoparticles in female Wistar rats after acute oral exposure. Mutagenesis 32 (4), 417–427.
Fischer, H.C., Chan, W.C., 2007. Nanotoxicity: the growing need for in vivo study. Curr. Opin. Biotechnol. 18 (6), 565–571.
Ge, S., et al., 2011. Cytotoxic effects of MgO nanoparticles on human umbilical vein endothelial cells in vitro. IET nanobiotechnology 5 (2), 36–40.
Gelli, K., et al., 2015. Assessment of pulmonary toxicity of MgO nanoparticles in rats. Environ. Toxicol. 30 (3), 308–314.
Gheshlaghi, Z.N., et al., 2008. Toxicity and interaction of titanium dioxide nanoparticles with microtubule protein. Acta biochimica biophysica Sinica 40 (9), 777–782.
Ghobadian, Mehdi, et al., 2015. Toxic effects of magnesium oxide nanoparticles on early developmental and larval stages of zebrafish (Danio rerio). Ecotoxicol. Environ. Saf. 122, 260–267.
Gómez, M., et al., 1997. The effect of age on aluminum retention in rats. Toxicology 116, 1–8.
Grissa, I., et al., 2015. Anemia and genotoxicity induced by sub-chronic intragastric treatment of rats with titanium dioxide nanoparticles. Mutat. Res. Genet. Toxicol. Environ. Mutagen 794, 25–31.
Gui, S., et al., 2011. Molecular mechanism of kidney injury of mice caused by exposure to titanium dioxide nanoparticles. J. Hazard. materials 195, 365–370.
Hashimoto, Kiyohiro, et al., 2010. An in vitro micronucleus assay with size-classified micronucleus counting to discriminate aneugens from clastogens. Toxicol. vitro 24 (1), 208–216.
He, F., et al., 2016. Redox mechanism of reactive oxygen species in exercise. Front. physiology 7 (486).
Heringa, Minne B., et al., 2016. Risk assessment of titanium dioxide nanoparticles via oral exposure, including toxicokinetic considerations. Nanotoxicology 10 (10), 1515–1525.
Hochella, Michael F., et al., 2008. Nanominerals, mineral nanoparticles, and earth systems. science 319 (5870), 1631–1635.
Hussein, S.A., et al., 2016. Curcumin ameliorates ethanol induced gastric mucosal erosion in rats via alleviation of oxidative stress and regulation of pro-inflammatory cytokines and NF-kappa B activation. Nat. Sci. 4 (4), 466–476.
Ivask, A., et al., 2015. DNA melting and genotoxicity induced by silver nanoparticles and graphene. Chem. Res. Toxicol. 28 (5), 1023–1035.
Jollow, D., et al., 1974. Bromobenzene-induced liver necrosis. Protective role of glutathione and evidence for 3, 4-bromobenzene oxide as the hepatotoxic metabolite. Pharmacology 11 (3), 151–169.
Karlsson, H.L., 2010. The comet assay in nanotoxicology research. Anal. Bioanal. Chem. 398 (2), 651–666.
Kiranmai, G., Reddy, A.R.N., 2013. Antioxidant status in MgO nanoparticle-exposed rats. Toxicol. industrial health 29 (10), 897–903.
Kongseng, Supunsa, et al., 2016. Cytotoxic and inflammatory responses of TiO2 nanoparticles on human peripheral blood mononuclear cells. J. Appl. Toxicol. 36 (10), 1364–1373.
Krishnamoorthy, K., et al., 2012. Mechanistic investigation on the toxicity of MgO nanoparticles toward cancer cells. J. Mater. Chem. 22, 24610–24617.
Kumaran, R.S., et al., 2015. In vitro cytotoxic evaluation of MgO nanoparticles and their effect on the expression of ROS genes. Int. J. Mol. Sci. 16 (4), 7551–7564.
Kumari, M., et al., 2013. Biochemical alterations induced by acute oral doses of iron oxide nanoparticles in Wistar rats. Drug Chem. Toxicol. 36 (3), 296–305.
Kumari, M., et al., 2014. Genotoxicity analysis of cerium oxide micro and nanoparticles in Wistar rats after 28 days of repeated oral administration. Mutagenesis 29 (6), 467–479.
Kumari, M., et al., 2014b. Toxicity study of cerium oxide nanoparticles in human neuroblastoma cells. Int. J. Toxicol. 33 (2), 86–97.
Lai, J.C., et al., 2008. Exposure to titanium dioxide and other metallic oxide nanoparticles induces cytotoxicity on human neural cells and fibroblasts. Int. J. Nanomed. 3 (4), 533–545.
Lee, I.-C., et al., 2016. Comparative toxicity and biodistribution assessments in rats following subchronic oral exposure to copper nanoparticles and microparticles. Part. fibre Toxicol. 13 (1), 56.
Liou, G.-Y., Storz, P., 2010. Reactive oxygen species in cancer. Free Radic. Res. 44 (5), 479–496.
Lobo, V., et al., 2010. Free radicals, antioxidants and functional foods: impact on human health. Pharmacogn. Rev. 4, 118–126.
López-Heras, I., et al., 2014. Prospects and difficulties in TiO 2 nanoparticles analysis in cosmetic and food products using asymmetrical flow field-flow fractionation hyphenated to inductively coupled plasma mass spectrometry. Talanta 124, 71–78.
Lowry, O.H., et al., 1951. Protein measurement with the Folin phenol reagent. J. Biol. Chem. 193, 265–275.
Mahmoud, A., et al., 2016. In vitro toxicological assessment of magnesium oxide nanoparticle exposure in several mammalian cell types. Int. J. Toxicol. 35 (4), 429–437.
Marklund, S., Marklund, G., 1974. Involvement of the superoxide anion radical in the autoxidation of pyrogallol and a convenient assay for superoxide dismutase. FEBS J. 47 (3), 469–474.
Martínez-Boubeta, C., et al., 2010. Ferromagnetism in transparent thin films of MgO. Phys. Rev. B 82, 024405.
McQueen, M., 1972. Optimal assay of LDH and α-HBD at 37° C. Ann. Clin. Biochem.

An Int. J. Biochem. Med. 9, 21–25.
Moeini-Nodeh, Shermineh, et al., 2017. Functional improvement in rats' pancreatic islets using magnesium oxide nanoparticles through antiapoptotic and antioxidant pathways. Biol. trace Elem. Res. 175 (1), 146–155.
Moorthy, S.K., et al., 2015. Synthesis and characterization of MgO nanoparticles by Neem leaves through green method. Mater. Today Proc. 2, 4360–4368.
Morsy, G.M., et al., 2016. Studies on fate and toxicity of nanoalumina in male albino rats: some haematological, biochemical and histological aspects. Toxicol. Ind. Health 32, 634–655.
Murdock, R.C., et al., 2008. Characterization of nanomaterial dispersion in solution prior to in vitro exposure using dynamic light scattering technique. Toxicol. Sci. 101 (2), 239–253.
Mylonas, C., Kouretas, D., 1999. Lipid peroxidation and tissue damage. vivo (Athens, Greece) 13, 295–309.
Oberdörster, G., et al., 2007. Toxicology of nanoparticles: a historical perspective. Nanotoxicology 1, 2–25.
OECD Guideline 420, 2001. Guideline for the Testing of Chemicals: Acute Oral Toxicity - Fixed Dose Procedure. Organization for Economic Cooperation and Development, Paris, pp. 1–14.
OECD Guideline 474, 2001. Mammalian Erythrocyte Micronucleus Test. Organization for Economic Cooperation and Development, Paris.
OECD Guideline 475, 2014. Mammalian Bone Marrow Chromosomal Aberration Test. Organization for Economic Cooperation and Development, Paris.
OECD Guideline 489, 2014. In Vivo Mammalian Alkaline Comet Assay. Organization for Economic Cooperation and Development, Paris.
Ohkawa, H., et al., 1979. Assay for lipid peroxides in animal tissues by thiobarbituric acid reaction. Anal. Biochem. 95, 351–358.
Ophardt, C.E., 2003. Denataration of Protein. Virtual Chembook. Elmhurst College.
Pant, K., et al., 2014. Vehicle and positive control values from the in vivo rodent comet assay and biomonitoring studies using human lymphocytes: historical database and influence of technical aspects. Environ. Mol. Mutagen. 55, 633–642.
Parivar, K., et al., 2016. Evaluation of iron oxide nanoparticles toxicity on liver cells of BALB/c rats. Iran. Red Crescent Med. J. 18 (1).
Pirela, Sandra V., et al., 2016. Effects of laser printer–emitted engineered nanoparticles on cytotoxicity, chemokine expression, reactive oxygen species, DNA methylation, and DNA damage: a comprehensive in vitro analysis in human small airway epithelial cells, macrophages, and lymphoblasts. Environ. health Perspect. 124 (2), 210.
Pool-Zobel, B.L., et al., 1994. Detection of genotoxic effects in human gastric and nasal mucosa cells isolated from biopsy samples. Environ. Mol. Mutagen. 24, 23–45.
Potapova, Tamara A., Zhu, Jin, Li, Rong, 2013. Aneuploidy and chromosomal instability: a vicious cycle driving cellular evolution and cancer genome chaos. Cancer Metastasis Rev. 32 (3–4), 377–389.
Reddy, U.A., et al., 2017. Biomarkers of oxidative stress for in vivo assessment of toxicological effects of iron oxide nanoparticles. Saudi J. Biol. Sci. 24 (6), 1172–1180.
Sahoo, S., et al., 2007. The present and future of nanotechnology in human health care. nanomedicine: nanotechnology. Biol. Med. 3 (1), 20–31.
Schmid, W., 1975. The micronucleus test. Mutat. Research/Environmental Mutagen. Relat. Subj. 31 (1), 9–15.
Shimizu, Noriaki, 2011. Molecular mechanisms of the origin of micronuclei from extrachromosomal elements. Mutagenesis 26 (1), 119–123.
Shrivastava, Rupal, et al., 2016. Oxidative stress following exposure to silver and gold nanoparticles in mice. Toxicol. industrial health 32 (8), 1391–1404.
Singh, S.P., et al., 2013a. Genotoxicity of nano-and micron-sized manganese oxide in rats after acute oral treatment. Mutat. Research/Genetic Toxicol. Environ. Mutagen. 754 (1), 39–50.
Singh, S.P., et al., 2013b. Toxicity assessment of manganese oxide micro and nanoparticles in Wistar rats after 28 days of repeated oral exposure. J. Appl. Toxicol. 33 (10), 1165–1179.
Singh, S.P., et al., 2013c. Comparative study of genotoxicity and tissue distribution of nano and micron sized iron oxidek in rats after acute oral treatment. Toxicol. Appl. Pharmacol. 266 (1), 56–66.
Sun, Jing, et al., 2011. Cytotoxicity, permeability, and inflammation of metal oxide nanoparticles in human cardiac microvascular endothelial cells. Cell Biol. Toxicol. 27 (5), 333–342.
Süzer, T., et al., 1999. Neuroprotective effect of magnesium on lipid peroxidation and axonal function after experimental spinal cord injury. Spinal Cord. 37 (7), 480–484.
Sycheva, L.P., et al., 2011. Investigation of genotoxic and cytotoxic effects of micro- and nanosized titanium dioxide in six organs of mice in vivo. Mutat. Research/Genetic Toxicol. Environ. Mutagen. 726, 8–14.
Thomas, B., et al., 2014. Comparative evaluation of serum antioxidant levels in periodontally diseased patients: an interventional study. Contemp. Clin. Dent. 5 (3), 340–344.
Tice, R., et al., 2000. Single cell gel/comet assay: guidelines for in vitro and in vivo genetic toxicology testing. Environ. Mol. Mutagen. 35, 206–221.
Wang, J., et al., 2007. Acute toxicity and biodistribution of different sized titanium dioxide particles in mice after oral administration. Toxicol. Lett. 168 (2), 176–185.
Yamakoshi, Yoko, et al., 2003. Active oxygen species generated from photoexcited fullerene (C60) as potential medicines: O2-• versus 1O2. J. Am. Chem. Soc. 125 (42), 12803–12809.
Yatzidis, H., 1960. Measurement of transaminases in serum. Nature 186, 79–80.
Zhang, H., et al., 2012. Use of metal oxide nanoparticle band gap to develop a predictive paradigm for oxidative stress and acute pulmonary inflammation. ACS Nano 6 (5), 4349–4368.
Zhang, L., et al., 2008. Nanoparticles in medicine: therapeutic applications and developments. Clin. Pharmacol. Ther. 83 (5), 761–769.
Zhang, L., et al., 2010. Mechanistic investigation into antibacterial behaviour of suspensions of ZnO nanoparticles against E. coli. J. Nanoparticle Res. 12, 1625–1636.